Seasonal and Across-Shelf Trends of the Phytoplankton Community of the Oregon Coastal Environment

by
Woody C. Moses and Patricia A. Wheeler
College of Oceanic and Atmospheric Sciences
Oregon State University

Data Report 194
COAS Reference 2004-2

A data report submitted to NEP-GLOBEC Long-term Observation Program.
For additional information please contact Patricia A. Wheeler (pwheeler@coas.oregonstate.edu)

ABSTRACT:

This project, part of the Northeast Pacific GLOBEC Long Term Observation Project (NEP-GLOBEC-LTOP), constitutes the first multi-year study of phytoplankton variability in the Oregon coastal environment. The work divides into two studies: analysis of interseasonal change and analysis of detailed changes within the summer upwelling period. In the first study, I found that the majority of variability in phytoplankton biomass in this system is due to changes in the abundance of chain forming diatoms, particularly diatoms of the genera *Chaetoceros* and *Skeletonema*. The abundance of nanoflagellates (<10 μm) remains constant across the shelf. They dominate the phytoplankton community in the offshore stations and larger cells, usually diatoms, are *added* inshore. Cyanobacteria, though numerically abundant, never comprise more than approximately 10% of phytoplankton biomass.

Variation within the summer phytoplankton bloom over the shelf was analyzed based on results from the four NEP-GLOBEC-LTOP summer cruises between August 1998 and July 2001. Nutrient concentrations during the summer upwelling blooms show a linear decrease with increasing temperature from 8 to 12° C. Over this range of temperatures, total Chl *a* and phytoplankton biomass increase, though not significantly, and the % Chl *a* >10 μm remains high (>50 %). Above 12° C, when inorganic nutrients are depleted or greatly reduced, total Chl *a* and % Chl *a* >10 μm decrease. The diatom genera *Chaetoceros* and *Skeletonema* are also responsible for the majority of the variability in phytoplankton stock during the summer phytoplankton bloom. Dinoflagellates, although present, are consistently less abundant than diatoms.

Section Table of Contents Page

Table of Contents, List of Figures and Tables **1**
Introduction **4**
The Oregon Coastal Environment and the Califonria Current System
The Importance of Phytoplankton Size and Diversity
Northeast Pacific GLOBEC-LTOP
Main Questions Considered
Methods **6**
Sample Collection
Physical Oceanographic Data
Biological Oceanographic Data
Inorganic Nutrients
Phytoplankton Identification and Biomass Estimation
Calculations and Statistical Analyses
Estimation of Euphotic Zone Depth and Integrated Chl *a*
Seasonal Groupings
Results **11**
Part I- Seasonal and Across-Shelf Environmental Variability
Upwelling and Hydrography During the Study
Seasonal and Across-Shelf Variation
Part II- The Summer Upwelling Phytoplankton Bloom **15**
Discussion **17**
Seasonal and Across-Shelf Environmental Variability
The Summer Upwelling Phytoplankton Bloom
Literature Cited **20**

Figures **22**

Appendix A: Data for all of the cruises, stations and depths used in this study. **49**
Appendix B: Numerical abundance of cyanobacteria, flagellates and diatoms. **91**
Appendix C: Biomass estimates of cyanobacteria, flagellates and diatoms. **93**
Appendix D: Numerical abundance of various sizes of unidentifiable diatoms. **95**
Appendix E: Numerical abundance estimates of various diatom genera. **97**
Appendix F: Biomass estimates of various sizes of unidentifiable diatom groups. **99**
Appendix G: Biomass estimates of various diatom genera. **101**
Appendix H: Biovolume estimates of phytoplankton cells. **103**

Figure List of Figures Page

1 PAR derived estimates of integrated Chl *a*.
2 Daily average upwelling index at 45˚N 125˚W.
3 Sea surface temperature and salinity.
4 Euphotic zone depth.
5 Integrated Chl *a* as a function of distance from shore.
6 % Chl *a* >10 μm as a function of distance from shore.
7 Integrated nitrate as a function of distance from shore.
8 July 2000 and 2001 across-shelf distribution of phytoplankton biomass.
9 July 2000 and 2001 across-shelf distribution of diatoms.
10 September 2000 across-shelf distribution of phytoplankton biomass.
11 September 2000 across-shelf distribution of diatoms.
12 January 2001 across-shelf distribution of phytoplankton biomass.
13 January 2000 across-shelf distribution of diatoms.
14 April 2000 and March 2001 across-shelf distribution of phytoplankton biomass.
15 April 2000 and March 2001 across-shelf distribution of diatoms.
16 Summer and September % Chl *a* >10 μm as a function of total Chl *a*.
17 Nutrient concentrations as a function of temperature.
18 Ammonium concentrations as a function of temperature.
19 Total Chl *a* and Chl *a* >10μm vs. temperature and % Chl *a* >10μm vs. total Chl *a*
20 Total Chl *a* as a function of nutrient concentrations.
21 % Chl *a* >10μm as a function of nutrient concentrations.
22 Chl *a* as a function of ammonium concentrations.
23 Distribution of biomass for the major groups of phytoplankton.
24 Cross shelf distribution of diatoms.
25 Chl and biomass of diatoms and flagellates vs. temperature

Table List of Tables Page

1 List of stations on the NH-Line sampled during this study. **7**
2 Means and coefficients of variation (C.V.) for inorganic nutrient samples. **8**
3 Shapes with corresponding equations of volume. **9**
4 Seasonal delineation of NEP GLOBEC-LTOP cruises used in the study. **11**
5 Upwelling index values. **11**
6. upwelling index values for first three days of each cruise. **12**
7. Euphotic zone depth, integrated Chl *a,* integrated nitrate and % Chl *a* > 10μm. **13**
8. ANOVA tables of multiple linear regressions analysis. **14**
9. Nutrients and Chl grouped by temperature. **16**

Introduction

This report is a documentation of the seasonal and across-shelf variability of the Oregon coastal phytoplankton community. The work divides into two studies: analysis of interseasonal change and examination of detailed changes within the summer upwelling period. Interseasonal variation is studied using data from seasonal cruises of the Northeast Pacific GLOBEC Long Term Observation Project (NEP-GLOBEC-LTOP), constituting the first multi-year study of phytoplankton variability in the Oregon coastal environment. Variation within the upwelling period is examined with greater resolution based on results from the four LTOP summer cruises between August 1998 and July 2001. Variability of phytoplankton composition during the upwelling period will be examined in light of the suite of simultaneous physical, chemical and biological measurements.

The Oregon Coastal Environment and the California Current System

The California Current strongly influences the Oregon coastal environment. This current flows equatorward along the west coast of North America, carrying colder, fresher, subarctic water with high oxygen and phosphate concentrations. The flow varies seasonally, with maximum velocities during the summer. During winter, the California Current moves offshore, replaced nearshore by the poleward flowing Davidson current, which consists of warmer, saltier, lower oxygen water (Huyer, 1983).

From May to September the Oregon coastal environment experiences predominantly upwelling-favorable conditions. During this time, there are a number of upwelling events lasting from two to 10 days, each characterized by offshore Ekman transport in the upper 20 m and onshore transport and shoaling of water from as deep as 150 m (Barber and Smith, 1981). The upwelling front, whose location corresponds to the outcropping of the 25.8σ_t isopycnal, is usually located between 10 and 15 km offshore (Austin and Barth, 2001). This front separates colder (8-12° C), nutrient-rich water inshore from warmer (>12° C), nutrient depleted water offshore (Peterson et al., 1979). Surface chlorophyll (chl) concentration changes, as does the structure of the phytoplankton community (Hood et al., 1992). During certain parts of the upwelling cycle, concentrations reach 3-6 μg/l inshore of the front, while offshore of the front, surface values are consistently less than 0.5 μg/l (Small and Menzies, 1981; Peterson et al., 2002).

From October to March, conditions along the Oregon coast are predominantly downwelling-favorable and the mixed layer reaches 50 to 80 m. During this time, surface chl is less than 1 μg/l right across the shelf (Hickey, 1989). The spring transition typically occurs between March and April, characterized by a decrease in the mixed layer depth and isopycnals that slope upward toward the shore (Smith et al., 2001). At the beginning of the transition, nutrient concentrations remain high from deep winter mixing, but they are soon depleted with the onset of the spring phytoplankton blooms, when chl increases strongly (Hickey, 1989).

The Oregon coastal environment is also influenced in the spring and summer by the Columbia River plume, a relatively fresh (<32 psu) lens of water between 5 and 20 m thick, usually located beyond the shelf break, beyond 50 km from shore. During the winter, the plume is carried north along the Washington coast and is compressed against the shore by prevailing winds. Hill and Wheeler (2002) found that the Columbia River plume water is relatively low in nitrate, but is a potentially important source of silicate to offshore water. The plume also contains high concentrations of total organic carbon (TOC) (up to 180 μM) and DOC (up to 150 μM), indicating that the Columbia River plume is a substantial source of organic carbon to the North Pacific Ocean.

The Importance of Phytoplankton Size and Diversity

Phytoplankton of different sizes dominate in different environments. Nanophytoplankton (<10 μm) contribute a greater fraction of total chl than do net-phytoplankton (>10 μm) in low nutrient regions, because they have a higher surface area relative to cell volume (Grover, 1989). For example, Booth et al. (1993**)** found at Station P in the subarctic Pacific that the 2-10 μm flagellates dominated the autotrophic community, and in a previous study (Booth, 1988) at the same location, it was determined that 39% of the autotrophic biomass was contributed by cells <2 μm. Furthermore, there tends to be a positive relationship between the total concentration of chl and the percent contribution of the net-phytoplankton to total phytoplankton standing stock (Chisholm, 1992).

Chain-forming diatoms are often the dominant net-phytoplankton in high nutrient, high chl coastal upwelling regions (Malone, 1980; Kokkinakis and Wheeler, 1988). The high levels of nutrients release these large phytoplankton from nutrient limitation, and because they grow up to three times faster than their competitors, diatoms outcompete other phytoplankton of equal size, that is dinoflagellates (Chisholm, 1992). The high growth rate of diatoms also reduces their relative loss to grazing and facilitates strong population growth (Strom et al., 2001).

Previous work shows that the Oregon coastal region follows this pattern. Kokkinakis and Wheeler (1988) found, during the summer, that chain-forming diatoms dominated in high nitrate areas, while small flagellates dominated in low nitrate areas. However, Hood et al. (1992) found, during early September, that *Synechococcus* spp., cryptomonads and small autotrophs (<10μm) dominated inshore of the upwelling front, an area usually of high nitrate concentrations. This project adds to these earlier studies by examining the seasonal changes in the phytoplankton community over the course of several years.

Studies on coastal phytoplankton blooms in temperate regions using enclosed experimental ecosystems have found that nitrate concentrations decrease as ammonium increases in the first stages of the bloom, but eventually both are depleted (Morris et al., 1985; Marrassé et al., 1989). Pitcher et al. (1993), working in the Benguela upwelling system, discovered that early bloom periods were cool (9.9-11° C), low in Chl *a* (0.01 – 0.31 μg/l), high in nutrients (nitrate: 12.6-26.6 μM), with seed stocks composed of either diatoms or small flagellates. As the bloom progressed, the changes in phytoplankton biomass were almost solely due to changes in the abundance of *Chaetoceros*, *Thalassiosira* and *Skeletonema*. These studies, conducted in microcosms, may not be completely accurate representations of natural systems. An *in situ* study, in the temperate coastal ecosystem of the Bay of Brest, France, found that the early spring bloom (April) was dominated by the diatom genera *Thalassiosira* and *Skeletonema*, the peak (May) by *Rhizosloenia*, and most diatoms were *Chaetoceros* at the end of the season (June) (Ragueneau et al., 1994). All of these studies suggest that the successional sequence of phytoplankton blooms is influenced by changes in environmental factors, such as temperature and nutrient concentration, as well as the phytoplankton community structure prior to bloom development.

Northeast Pacific GLOBEC-LTOP

The relatively narrow (~40 km) continental shelf off Oregon facilitates sampling both nearshore and in open ocean environments over the course of several hours. Since August 1997, NEP GLOBEC-LTOP has been measuring the large-scale distribution of physical, chemical and biological parameters in this system from central Oregon to Northern California. These parameters are temperature, salinity, fluorescence, oxygen, inorganic nutrient concentrations, particulate and dissolved organic carbon and nitrogen, and both total and size-fractionated chl. Sampling is seasonal, with approximately five cruises per year. It covers the shelf (0 to 37 km from shore; 0 to 200 m deep), slope (37 to 84 km from shore; 200 to 700 m deep) and offshore (84 to 157 km from shore; >700 m deep) environments.

We utilized temperature, salinity, chl (total and size fractionated) and inorganic nutrient measurements collected during cruises from August 1998 to July 2001. Data from earlier cruises are considered to have occurred during the 1997-98 El Niño and were excluded from consideration. Furthermore, only data from the northern-most transect, the NH-Line, were used in this study, because it is the only transect sampled consistently throughout the year. In addition to these measurements, I collected samples for microscopic analysis during six cruises between April 2000 and July 2001, which allowed taxonomic analysis of the phytoplankton community.

We characterized the stages of the summer phytoplankton bloom by examining the relationship between temperature and inorganic nutrient concentrations of shelf samples collected during four summer cruises and three September cruises between August 1998 and July 2001 (August 1998, September 1998 July 1999, September 1999, July 2000, September 2000 and July 2001). Because inorganic nutrients (nitrate, phosphate and silicate) decrease and temperature increases with time since upwelling, one can determine the relative age of upwelled water by correlating these parameters. Using that relationship, I defined various stages in the progression of the bloom. Total and size-fractionated chl were then used to determine the relative contribution of nano- and net-phytoplankton to total phytoplankton standing stock for each stage of the bloom, and microscopy was implemented to determine the taxonomic composition of phytoplankton over the course of the bloom. The temperature, salinity, chl and inorganic nutrient data used in this study can be found in Appendix A, while the full dataset can be accessed at the NEP GLOBEC-LTOP web site (http://ltop.oce.orst.edu). The phytoplankton biomass and numerical abundance data are in Appendices B through G, and the phytoplankton biovolume data is in Appendix H.

Main Questions Considered

We attempted to answer the questions: "How do the biomass, size structure and diversity of the phytoplankton community vary seasonally and with distance from shore off the Oregon coast?" and "How do inorganic nutrient concentrations, temperature, phytoplankton biomass, size fractionation and taxonomic community diversity change over the course of a summer phytoplankton bloom off the Oregon coast?". Based on previous work in these waters by Peterson et al. (1981), Kokkinakis and Wheeler (1988) and Corwith and Wheeler (2002), I predicted that total chl and % chl >10 µm would show strong seasonal variability. Both total chl and % chl >10 µm were expected to be highest over the shelf during the summer upwelling season, when the phytoplankton community is dominated by chain-forming diatoms, and to be lowest during the winter, when the phytoplankton community would be dominated by small flagellates. During the progression of the summer phytoplankton bloom, I predicted that total chl and % chl >10 µm would increase with temperature, while nutrients would be depleted and chain-forming diatoms would dominate (Morris et al., 1985; Marrassé et al., 1989; Pitcher et al., 1993 and Ragueneau et al., 1994). The late bloom would be characterized by depleted nutrients, and chl and % chl >10 µm would be relatively low because conditions would be more oligotrophic (Chisolm, 1992).

Methods

Sample Collection. NEP-GLOBEC-LTOP collected samples during 15 cruises on the R/V Wecoma from August 1998 to July 2001 along the Newport Hydroline (NH-Line), a transect extending westward from Yaquina Head at 44˚39.1'. Samples were collected at from 7 to 11 stations, varying in distance from 5 to 157 km from shore. Stations NH-05, 15, 25, 35, 45, 65 and 85 are permanent NEP-GLOBEC-LTOP stations and were sampled throughout the study. Stations NH-03, 10, 20 and 55 are only used in this project for taxonomic phytoplankton classification and were only sampled from April 2000 to July 2001. The station numbers refer to the distance of the station from shore in nautical miles. Table 1 contains a log of station information.

Table 1: List of stations of Newport Hydroline (44˚39.1' N), study for which they were sampled, environment in which they are located, longitude, km from shore, station depth, and depths sampled at each station.

Station	Study	Environment	Longitude	km	Depth (m)	Depths Sampled (m)
NH-03	This Project	Shelf	124˚08' W	5	48	Surface and Chl Max
NH-05	LTOP	Shelf	124˚11' W	9	60	Surface, 5, 10, 15, 20, 25, 30, 40, 50, 55, and Chl Max
NH-10	This Project	Shelf	124˚18' W	18	80	Surface and Chl Max
NH-15	LTOP	Shelf	124˚25' W	28	90	Surface, 5, 10, 20, 30, 40, 50, 60, 70, 85 and Chl Max
NH-20	This Project	Shelf	124˚32' W	37	140	Surface and Chl Max
NH-25	LTOP	Slope	124˚39' W	46	296	Surface, 10, 20, 30, 40, 50, 70, 100, 150, 200 and Chl Max
NH-35	LTOP	Slope	124˚53' W	65	435	Surface, 10, 20, 30, 40, 50, 70, 100, 150, 500 and Chl Max
NH-45	LTOP	Slope	125˚07' W	84	700	Surface, 10, 20, 30, 40, 50, 70, 100, 150, 500 and Chl Max
NH-55	This Project	Offshore	125˚22' W	102	2885	Surface and Chl Max
NH-65	LTOP	Offshore	125˚36' W	120	2880	Surface, 10, 20, 30, 40, 50, 70, 100, 150, 1000 and Chl Max
NH-85	LTOP	Offshore	126˚03' W	157	2900	Surface, 10, 20, 30, 40, 50, 70, 100, 150, 1000 and Chl Max

Physical Oceanographic Data. Temperature and salinity data were collected with a Sea-Bird 9/11-plus CTD system equipped with dual-ducted temperature and conductivity sensors. All physical oceanographic data can be found in Fleischbein et al. (1999) or at the NEP GLOBEC LTOP web site: (http://ltop.oce.orst.edu).

Biological Oceanographic Data. Chl samples for determining euphotic zone depth and integrated Chl *a* were taken from all depths less than 150 m at all permanent NEP-GLOBEC-LTOP stations. Samples for determining Chl *a* in the >10 μm fraction were collected from the surface (0.5 to 3 m depth), 10 m and in the subsurface chl maximum of permanent NEP-GLOBEC-LTOP stations. Stations NH-03, 10, 20 and 55 were only sampled at the surface and in the subsurface chl maximum. Duplicate samples for total chl and chl >10 μm were collected at these depths, except in April 2000 when no chl samples were taken at these stations and in July 2000, when only total chl samples were collected at these stations. The depth of the subsurface chl maximum was determined from the fluorescence maximum indicated by the *in situ* fluorometer on the CTD. For measurements of total chl, 154 ml of seawater were filtered through pre-combusted 25mm Whatman™ GF/F filters using vacuum filtration at pressures less than 8 psi. In order to estimate the chl of cells greater than 10 μm, 100 ml of seawater from the same Niskin bottle were prefiltered through a 10 μm Nitex screen before filtering onto a GF/F filter, removing cells >10 μm. The

chl of cells >10 μm was calculated as the difference between the total chl and the chl of cells <10 μm. The GF/F filters were stored in a dark freezer in glass tubes until they were processed back on shore.

Pigments were extracted from these samples in 10 ml of 95% HPLC grade methanol (5% DIW) for at least 12 h, but no longer than 48 h, in plastic centrifuge tubes in a dark freezer. The extracted chl concentrations were determined fluorometrically, using a Turner Designs™ 10-AU fluorometer. The instrument was calibrated yearly using a powdered *Anacystis nidulans* Chl *a* standard (Sigma®) dissolved in 95% HPLC grade methanol (Parsons et al., 1984).

Inorganic Nutrients. Inorganic nutrient samples were also collected at each of the above depths. I sampled for inorganic nutrients at NH-03, 10, 20 and 55 during every cruise, except April 2000. For March and July 2001 cruises, duplicate samples were collected in 30 ml HDPE bottles at each depth, as opposed to single samples in 60 ml HDPE bottles as were collected on earlier cruises. All samples were frozen immediately and remained frozen until processing. They were analyzed for nitrate, nitrite, ammonium, silicate, and phosphate using a continuous flow Technicon™ AutoAnalyzer-II ™ according to the methods of Gordon et al. (1995).

Mean concentrations and corresponding coefficients of variation for duplicate inorganic nutrient samples from the March and July 2001 cruises are found in Table 2. The average coefficient of variation of duplicate samples taken during the March 2001 cruise were 1.62% for phosphate, 33.7% for ammonium, 10.5% for silicate, and 1.85% for nitrate. The mean coefficients of variation for the July 2001 cruise were 4.2% for phosphate, 54.6% for ammonium 10.91% for silicate, and 5.4% for nitrate. At the time of writing this report, full depth profiles of inorganic nutrient data, particularly nitrate concentrations, were not available for January, March and July 2001 cruises, and therefore integrated nitrate values from those cruises are not included in this report.

Table 2: Means (μM) and coefficients of variation (C.V.) for duplicate inorganic nutrient samples taken during the March and July 2001 cruises. ND indicates missing data.

		Depth	Phosphate		Ammonium		Silicate		Nitrate	
Cruise	**Station**	**(m)**	**Mean**	**C.V.**	**Mean**	**C.V.**	**Mean**	**C.V.**	**Mean**	**C.V.**
Mar-01	**NH-03**	3	0.41	1.24	0.25	114.00	0.00	4.13	0.00	0.07
		23	0.39	5.53	0.14	58.00	0.00	3.87	0.00	0.09
	NH-10	1	0.48	0.05	0.20	6.24	0.45	25.06	0.83	0.52
		65	0.48	0.05	0.20	3.22	0.51	21.90	1.06	6.04
	NH-20	1	0.57	ND	ND	ND	3.64	ND	3.28	ND
		10	0.57	0.04	0.02	12.60	4.53	14.64	3.46	2.15
	NH-55	1	0.59	4.39	0.15	29.54	3.17	2.10	3.67	3.83
		19	0.60	0.04	0.16	12.60	3.36	1.98	3.63	0.26
Jul-01	**NH-03**	1	2.66	4.78	0.24	7.05	51.90	6.06	31.20	5.70
		11	2.75	1.10	0.43	32.78	52.90	0.02	31.95	0.13
	NH-10	1	2.05	1.54	0.93	71.40	28.93	3.70	22.12	3.65
		13	2.08	2.01	0.73	44.70	29.95	3.74	29.95	3.42
	NH-20	1	0.87	5.11	0.46	55.74	5.36	7.50	6.02	7.60
		26	1.44	8.87	0.31	25.85	14.24	13.35	13.68	13.38
	NH-55	1	0.25	9.20	0.06	179.02	0.00	41.30	0.00	0.53
		45	0.61	1.14	0.12	20.06	1.15	11.62	0.54	8.45

Phytoplankton Identification and Biomass Estimation. The surface and subsurface chl maximum of stations NH-03, 10, 20 and 55 were sampled for phytoplankton identification and biomass estimates during the following cruises: April, July and September 2000, and January, March and July 2001. Duplicate samples for both 0.8 μm and 1.0 or 3.0 μm black PC membrane filters were taken from each Niskin bottle. During the first two cruises, I used 3.0 μm filters, but because the production of 3.0 μm membrane filters was discontinued during the project, I switched to 1.0 μm membrane filters. The 0.8 μm filters were used for counting cyanobacteria (~1.0 μm), while the 1.0 μm and 3.0 μm filters were used for counting larger phytoplankton. Samples were collected as described by Sherr et al. (1993). Duplicate 250 ml samples were taken at each depth and fixed using 6 ml of borate buffered formalin, three drops of alkaline Lugols solution and six drops of sodium thiosulfate and were refrigerated for at least six, but no longer than 48 h, in order to harden the cells. They were then filtered through the membrane filters using vacuum filtration with pressures less than 8 psi I filtered 150 ml of each sample through 1.0 or 3.0 μm membrane filters and 50 ml of the same sample through 0.8 μm filters. During the filtration process a 500 μg/ml DAPI solution was added to the samples in order to distinguish between living material and detritus. Filters were mounted on glass slides using immersion oil and frozen at temperatures below -20º C until analysis.

Cells were counted using epifluorescent microscopy. we counted all non-detrital phytoplankton cells in a field and performed surveys to quantify different size classes. For the cyanobacteria, I counted all of the cells in ten random fields at 1000x magnification, using only the 0.8 μm filters. Phytoplankton between 1 and 20 μm were counted in 30 random fields at 1000x magnification. I only counted phytoplankton smaller than 10 μm using the 0.8 μm filters, while I used only the 1.0 or 3.0 μm filters for phytoplankton between 10 and 20 μm. For cells larger than 20 μm, I used 160 x magnification and counted either the entire slide or, if the total number of cells was greater than 400, I counted half of it. I used 0.8 μm filters for samples with more than 400 >20 μm phytoplankton on a filter because they represented only 50 ml of sample. I used 1.0 or 3.0 μm filters, representing 150 ml, when the total number of phytoplankton was less than 400.

We grouped cells taxonomically as cyanobacterium, flagellate or diatom. I identified diatoms to genus when possible, and when it was not I classified them as chain-forming, single, single centric or pennate. Cells were sized and shaped in order to convert to biovolume. Table 3 lists the shapes used in this study along with the equation used to determine biovolume. If the shape was not distinguishable, I used a spherical approximation with the shortest axis of the cell as the diameter of the sphere.

Table 3: Shapes with corresponding equations of volume.

Shape	**Equation of Volume**
Sphere	$(4/3)\pi r^3$
Cylinder	$(\pi r^2)h$
Cone	$1/3(\pi r^2)h$
Oblate Spheroid	$4/3\ (A/2)^2(B/2)$
Teardrop	$4/3(\pi r^2)h + 2/3(\pi r^2)$

Carbon estimates were calculated from biovolume using the equations of Strathmann (1967):

Diatoms: Log C (pg/cell) = -0.422 + 0.758 * log Avg. Cell Volume (μm^3/cell)

Flagellates: Log C (pg/cell) = -0.460 + 0.866 * log Avg. Cell Volume (μm^3/cell)

Carbon equivalents for the cyanobacteria were derived using Booth's (1988) equation for phytoplankton of 1 to 4 μm:

Carbon (pg/cell) = 0.22 (pg/μm^3) * Avg. Cell Vol (μm^3/cell)

Calculations. The concentration of Chl *a* contributed by cells greater than 10 μm (Chl *a* >10 μm) was calculated by subtracting the Chl *a* concentration of prefiltered samples from that of whole water samples. I calculated maximum and minimum estimates of Chl *a* > 10 μm using the maximum and minimum estimates for the duplicate total Chl *a* and Chl *a* <10 μm samples using the following equations:

$$\text{Chl } a > 10\ \mu m_{max} = \text{Total Chl}_{max}\ a - \text{Chl } a < 10\ \mu m_{min}$$
$$\text{Chl } a > 10\ \mu m_{min} = \text{Total Chl}_{min}\ a - \text{Chl } a < 10\ \mu m_{max}$$

Maximum and minimum estimates of percent chl in the > 10 μm fraction (% Chl *a* >10 μm) were calculated using the above estimates and the following equations:

$$\%\ \text{Chl } a > 10\ \mu m_{max} = \text{Chl } a > 10\ \mu m_{max} / \text{Total Chl}_{min}\ a$$
$$\%\ \text{Chl } a > 10\ \mu m_{min} = \text{Chl } a > 10\ \mu m_{min} / \text{Total Chl}_{max}\ a$$

If the <10 μm (prefiltered) sample contained more chl than the whole sea water sample, the <10 μm fraction was considered to be 100% of the total Chl *a*.

Statistical Analyses. Effects of distance from shore on euphotic zone depth, integrated Chl *a*, % Chl *a* >10 μm and integrated nitrate in lieu of seasonal and interannual variability were estimated by multiple linear regression using a general linear model (S.A.S.® statistical package). Significance of seasonal differences in the above variables at nearshore stations was determined using ANOVA (SPSS® statistical package). Simple linear regressions were performed using Excel®, and all t-tests were calculated by hand.

Estimation of Euphotic Zone Depth and Integrated Chl *a*. The depth of the euphotic zone was assumed to be where ambient light levels equaled 1% of surface irradiance. Because the majority of CTD casts did not have a PAR sensor it was necessary to estimate the extinction coefficient of light, from which we could determine the depth of the 1% light level. The extinction coefficient for light penetration was calculated as $k = 0.04 + 0.0088C + 0.054C^{2/3}$ (Riley, 1956), where 0.04 is the extinction coefficient of light in pure sea water and C is the concentration of Chl *a*. This estimate of euphotic zone depth was used by Small and Curl (1968), who found good agreement between these estimates and measured euphotic zone depth. Chl *a* concentrations were integrated to the base of the euphotic zone, which was considered to be the depth, z, where k*z = 4.6. Estimates of k were made using an iterative process developed by Spitz and Corwith (see Corwith, 2000) in which chl profiles were integrated in 1 m increments, and a k value was estimated for each. Maximum and minimum integrated chl values were estimated for each depth profile by using the highest and lowest total chl values of duplicate samples.

A comparison (Fig.1) between integrated Chl *a* values obtained using PAR sensor estimates of euphotic zone depth and values of integrated Chl *a* from euphotic zone depths estimated using Riley's equation had a high r^2 (0.9902) and a slope near one (y=1.0692x-3.4128). Both suggest that Riley's equation agrees with PAR sensor estimates of euphotic zone depth. Furthermore, the correlation between the two estimates is greatest at high (>50 mg/m^2) levels of integrated Chl *a*. These high values came from shelf stations, which are the focus of much of the research in the Oregon coastal upwelling environment.

Seasonal Groupings. Cruises were grouped by season based upon large-scale, interseasonal differences in hydrographic parameters, such as upwelling versus downwelling favorable conditions. The upwelling index at 45º N 125º W for August 1998 to July 2001 was calculated by P.F.E.L. (Pacific Fisheries Environmental Laboratory) from wind stress along the Oregon coast using Ekman's transport theory (Fig. 2). Table 4 lists the seasonal groupings of the various cruises.

Table 4: Seasonal groupings of NEP GLOBEC-LTOP cruises.	
Season	**Cruises**
Summer	August 1998, July 1999, July 2000, July 2001
September	September 1998, September 1999, September 2000
Winter	November 1998, January 1999, November 1999, February 2000, January 2001
Spring	April 1999, April 2000, March 2001

Results. Part I- Seasonal and Across-Shelf Environmental Variability

Upwelling and Hydrography During the Study. A consistent seasonal pattern of upwelling during the summer and strong downwelling during the winter is evident from January 1990 to October 2001, including the period of this study, August 1998 to July 2001 (Fig. 2). Table 5 lists mean upwelling index values during the five days prior to each cruise, the three days at the beginning of each cruise and the next five days after the first three days of each cruise. It is important to note that even though upwelling conditions are variable on the order of days, as is illustrated by the high standard deviations, they are consistent before during and after each cruise (Table 5).

Mean upwelling index values averaged over the first three days of each cruise (when the NH-Line was sampled) correspond to seasonal differences in upwelling conditions (Table 6). Summer (July and August) cruises coincide with predominantly upwelling conditions, while winter cruises (November and January/February) coincide with predominantly downwelling conditions. It should also be noted that upwelling does occur in winter, which is suggested by the large standard deviation relative to the mean

Table 5: Mean and standard deviation of upwelling index values in $m^3s^{-1}100m^{-1}$ measured at 45ºN 125ºW for each of the cruises in this study. Cruises are grouped by the season in which they occurred.

		Upwelling Index					
		5 Days Prior		**3 Days During**		**Next 5 Days**	
Season	**Cruise**	**Mean**	**SD**	**Mean**	**SD**	**Mean**	**SD**
Summer	**Aug-98**	77	20	86	17	45	33
	Jul-99	37	30	19	7	42	19
	Jul-00	26	25	56	1	56	37
	Jul-01	117	68	57	8	120	20
September	**Sep-98**	43	14	43	14	54	24
	Sep-99	62	13	27	4	40	15
	Sep-00	9	22	16	23	15	22
Winter	**Nov-98**	-165	115	-34	68	-230	201
	Feb-99	-272	237	-180	79	-322	249
	Nov-99	-7	72	-38	71	-215	196
	Feb-00	-132	146	-264	352	-164	80
	Jan-01	-127	137	-41	71	-95	103
Spring	**Apr-99**	17	73	5	24	70	50
	Apr-00	6	15	7	8	23	44
	Mar-01	-50	56	60	57	-58	103

Table 6: Mean(SD) upwelling index values for the first three days of each cruise (when the NH-Line was sampled) are grouped by season. This table also includes mean surface temperature and salinity conditions in the shelf, slope and offshore (O.S.) regions taken from cruises during each season.

	Upwelling Index	Surface Temperature(ºC)			Surface Salinity (psu)		
	($m^3 s^{-1} 100 m^{-1}$)	Shelf	Slope	O.S.	Shelf	Slope	O.S.
Summer	55 (32)	12.0 (2.0)	15.1(2.3)	16.1(2.7)	31.3(1.8)	30.3(1.6)	30.9(0.9)
September	29 (86)	12.1 (2.0)	15.3(4.2)	15.1(2.1)	32.6(0.5)	32.0(0.3)	32.1(0.4)
Winter	-111 (557)	10.4 (1.2)	10.8(1.2)	11.2(1.8)	32.5(0.3)	32.6(0.1)	32.5(0.1)
Spring	24 (72)	10.3 (0.5)	10.3(0.5)	10.1(0.8)	31.8(0.7)	31.9(0.9)	32.6(0.3)

upwelling index value, but the mean is still negative (-111 ± 557 $m^3 s^{-1} 100 m^{-1}$). The spring (April and March) and September cruises coincide with the transition period between predominantly upwelling and predominantly downwelling conditions, as is seen in the smaller mean upwelling index and the large standard deviation. The mean upwelling index for both these seasons is positive, but the standard deviation is larger than the mean, indicating that these seasons experience both upwelling and downwelling (spring: 24 ± 72 $m^3 s^{-1} 100 m^{-1}$ and September: 29 ± 86 $m^3 s^{-1} 100 m^{-1}$).

Seasonal and across shelf patterns in temperature and salinity were used to characterized the prevalent water masses during each season (Fig. 3; Table 6). The summer season is characterized by three different water masses: 1) the cold (12.0 ± 2.0˚ C), salty (31.3 ± 1.8 psu) upwelled water over the shelf 2) warmer (15.1 ± 2.3˚ C), fresher (30.3 ± 1.6 psu) water mostly over the slope that is influenced by the Columbia River plume and 3) the warmer (16.1 ± 2.7˚ C), North Pacific surface water, that tends to be saltier (30.9 ± 0.9 psu) and farther offshore than the Columbia River plume. September is very similar to summer, but higher salinity over the slope suggests that the river plume is farther offshore. Winter salinity is relatively constant across the shelf, and spring is characterized by relatively constant temperature across the shelf (Figure 3; Table 6).

Seasonal & Across-Shelf Variation in Euphotic Zone Depth, Integrated Chl *a* & NO_3^-.

Euphotic zone depth, integrated Chl *a* and % Chl *a* >10 μm all show seasonal variability in their across-shelf distributions (Figs. 4-6; Table 7), and this variability is greatest in the shelf region (< 28 km from shore). Overall, euphotic zone depth increased significantly across the shelf (Fig. 4; Table 8), despite significant seasonal and interannual variability ($F_{(2,303)}$=94.66, p<0.0001). Summer had the shallowest euphotic zone depth nearshore (34 ± 18 m), which was significantly shallower (p<0.05, t = 3.10 df = 17) than during the winter (54 ± 10 m). However, an ANOVA indicated no significant difference (p = 0.861, $F_{(2,19)}$ = 0.15) from September (39 ± 14 m) or spring (36 ± 18 m) (Fig. 4).

Overall, integrated Chl *a* and % Chl *a* >10 μm decreased significantly with distance from shore, despite significant seasonal and interannual variability (integrated Chl *a*: $F_{(2,303)}$ = 115.29, p<0.0001; % Chl *a* >10 μm: $F_{(2,232)}$ = 31.69, p<0.0001) (Figs. 5,6; Table 8). An ANOVA indicated no significant difference in % Chl *a* >10 μm among the three sampling depths, the surface, 10 m and subsurface chl maximum (p = 0.10, $F_{(46,276)}$ = 1.315). Summer in the shelf region had the highest mean integrated Chl *a* (70 ± 44 mg/m^2) and % Chl *a* >10μm (64 ± 28 %) (Fig. 4). These were significantly greater (integrated. Chl *a*: p<0.05, t = 2.67 df =16; % Chl *a* >10 μm: p<0.05, t = 4.99 df = 50) than during the winter (Int. Chl *a*: 32 ± 10 mg/m^2; % Chl *a* >10 μm: 28 ± 24%), though an ANOVA found them not to be significantly different (integrated Chl *a*: p = 0.80, $F_{(2,19)}$ = 0.228; % Chl *a* >10μm: p = 0.07, $F_{(2,52)}$ = 2.86) from either September or spring (Figs. 5,6; Table 7).

Integrated nitrate decreased significantly with distance from shore ($F_{(2,81)} = 3.68$, $p<0.0298$) and interannually ($F_{(3,281)} = 5.89$, $p = 0.0042$), but did not differ significantly by season ($F_{(3,232)} = 1.50$, $p<0.2218$) (Fig. 7; Table 7). The highest mean integrated nitrate values were found during summer over the shelf (501 ± 487), but an ANOVA indicated that they were not significantly different from nearshore values in any other season ($p = 0.232$, $F_{(3,24)} = 1.548$) (Table 7).

Table 7: Mean and SD of euphotic zone depth, integrated Chl *a* and nitrate, and % Chl *a* >10 μm during each season in the shelf, slope and offshore regions.

		Euphotic Depth (m)	Int. Chl *a* (mg/m^2)	Int. NO3 ($mmol/m^2$)	%Chl>10um
Summer	**Shelf**	34 (18)	70 (44)	501 (487)	64 (28)
	Slope	57 (12)	31 (12)	214 (148)	19 (19)
	Offshore	67 (13)	22 (9)	91 (42)	24 (23)
September	**Shelf**	39 (14)	57 (22)	456 (258)	40 (36)
	Slope	66 (16)	27 (13)	403 (339)	12 (18)
	Offshore	62 (6)	28 (7)	240 (196)	16 (21)
Winter	**Shelf**	54 (10)	32 (10)	395 (129)	28 (24)
	Slope	59 (7)	29 (6)	350 (161)	14 (15)
	Offshore	61 (14)	21 (10)	234 (96)	17 (18)
Spring	**Shelf**	36 (18)	62 (26)	132 (37)	43 (34)
	Slope	62 (20)	28 (15)	312 (212)	8 (7)
	Offshore	65 (13)	21 (6)	262 (34)	14 (10)

Across-Shelf Distribution of Phytoplankton During Each Season. Estimated numerical abundances of the major groups of phytoplankton are listed in Appendix B, while the numerical abundances of unidentified diatoms and identifiable diatom genera are listed in Appendices D and E respectively. Biomass estimates of the major groups of phytoplankton are listed in Appendix C, while the biomass estimates of unidentified diatoms and identifiable diatom genera are listed in Appendices F and G, respectively.

Summer. During the July 2000 cruise, total phytoplankton biomass at the surface and in the subsurface chl maximum was highest at NH-03 and decreased offshore. Surface total phytoplankton biomass was significantly greater at NH-3 (137 ± 55 μgC/l) than at NH-55 (9.05 ± 0.43 μg C/l) ($p< 0.05$, $t = 3.28$ df =2). At both NH-03 and NH-10, the surface phytoplankton community was dominated by diatoms between 10 and 20 μm, with concentrations of 108 ± 41 and 41 ± 0.28 μg C/l respectively (Fig. 8). Large diatom cells became much less abundant offshore. By NH-20 and 55, the phytoplankton community was dominated by flagellates between 1 and 10 μm, whose biomass remained relatively constant across the shelf (Fig. 8), suggesting that changes in phytoplankton biomass across the shelf were driven by almost entirely by changes in the abundance of diatoms. Cyanobacteria, though numerically abundant, were never the dominant group of phytoplankton in terms of carbon biomass (Fig. 8). The most abundant diatom genus at NH-03 and 10 was *Chaetoceros*, which comprised approximately 84% of the diatom biomass in the surface at NH-03 (Fig. 9). The abundance of *Chaetoceros* decreased from nearshore to offshore, suggesting that the changes in diatom biomass, and therefore total phytoplankton biomass, are determined by this genus.

Table 8: Multiple linear regression analyses of A. euphotic zone depth B. integrated Chl *a* C. % Chl *a* >10 μm and D. integrated nitrate as a function of distance from shore, season and year of the study.

A. Euphotic Zone Depth

Source	DF	Sum of Squares	Mean Square	F Value	Pr > F
Model	14	53880	3849	27.82	<**0.0001**
Error	289	39990	139		
Corrected Total	303	93870			

Source	DF	Type III SS	Mean Square	F Value	Pr > F
Dist. From Shore	2	26190	13100	94.66	**<0.0001**
Season	3	3429	1143	8.26	**<0.0001**
Year	3	17040	5680	41.05	**<0.0001**

B. Integrated Chl *a*

Source	DF	Sum of Squares	Mean Square	F Value	Pr > F
Model	14	116600	8331	34.91	**<0.0001**
Error	289	68960	238		
Corrected Total	303	185600			

Source	DF	Type III SS	Mean Square	F Value	Pr > F
Dist. From Shore	2	55020	27510	115.29	**<.0001**
Season	3	13670	4556	19.09	**<.0001**
Year	3	31930	10640	44.60	**<.0001**

C. % Chl *a* >10 μm

Source	DF	Sum of Squares	Mean Square	F Value	Pr > F
Model	13	114.6	8.815	9.72	**<0.0001**
Error	219	198.6	0.907		
Corrected Total	232	313.2			

Source	DF	Type III SS	Mean Square	F Value	Pr > F
Dist. From Shore	2	57.48	28.74	31.69	**<0.0001**
Season	3	29.12	9.71	10.70	**<0.0001**
Year	3	9.36	3.12	3.44	**0.0177**

D. Integrated nitrate

Source	DF	Sum of Squares	Mean Square	F Value	Pr > F
Model	7	1268147	181164	4.11	**0.0007**
Error	74	3262128	44082		
Corrected Total	81	4530275			

Source	DF	Type III SS	Mean Square	F Value	Pr > F
Dist. From Shore	2	324810	162404	3.68	**<0.0298**
Season	3	198290	66097	1.50	**0.2218**
Year	3	519350	259675	5.89	**0.0042**

In July 2001 total phytoplankton biomass was greater at NH-10 (55.5 ± 59.9 μgC/l) than NH-03 (29.5 ± 22.3 μgC/l), though not significantly so ($p>0.05$, $t = 0.58$ $df=2$) (Fig. 8). The peak in biomass at NH-10 corresponded to both the peak in diatom biomass and to the peak in relative abundance of *Chaetoceros*, providing further evidence that changes in phytoplankton biomass are strongly influenced by this genus (Fig. 9).

September. During the September 2000 cruise, total phytoplankton biomass again decreased significantly ($p<0.05$, $t = 2.98$ $df = 2$) onshore to offshore from 26.4 ± 11.4 μgC/l in the surface at NH-03 to 2.6 ± 1.8 μgC/l in the surface at NH-55 (Fig. 10). However, flagellates <20 μm were the dominant group of phytoplankton both nearshore and offshore. Diatoms were only abundant at NH-10, where the biomass of diatoms 10-20 μm (8.6 ± 11.5 μgC/l) was not significantly different ($p>0.05$, $t = 0.24$ $df = 2$) from that of flagellates <10 μm (10.7 ± 5.5 μgC/l). Of the diatoms present, *Chaetoceros* was the most abundant, particularly at NH-03 and NH-10 in the surface and at NH-55 in the subsurface chl maximum. In the surface, at both NH-20 and NH-55 the diatom community was dominated by a few large single centric diatoms >20 μm (Fig. 11).

Winter. During the January 2001 cruise, total phytoplankton biomass in both the surface and subsurface chl maximum remained relatively constant across the shelf, while the composition of the phytoplankton community changed (Fig. 12). In the surface at NH-03, the biomass of diatoms 10-20 μm (1.88 ± 0.00 μgC/l) did not differ significantly from ($p>0.05$, $t = 2.10$ $df=2$) that of flagellates <10 μm (1.48 ± 0.27 μgC/l). However, diatom biomass was almost negligible at both NH-20 (0.06 ± 0.07 μgC/l) and NH-55 (0.00 ± 0.00 μgC/l), and flagellates <10 μm dominated (Fig. 12). Of the diatoms present, *Chaetoceros*, *Skeletonema*, and *Thalassiosira* were dominant at NH-03 and NH-10, both in the surface and in the subsurface chl maximum (Fig. 13). In the subsurface chl maximum at NH-20 and NH-55 and in the surface at NH-20, unidentified single centric diatoms >20 μm dominated, while in the surface at NH-55 *Chaetoceros* dominated.

Spring. Both the April 2000 and the March 2001 cruises showed the same across shelf trend in total phytoplankton biomass as the summer and September cruises; phytoplankton biomass was highest over the shelf (NH-03 and NH-10), and decreased offshore. The trend was consistent at both the surface and the subsurface chl maximum (Fig. 14). The high biomass stations were dominated by diatoms, particularly diatoms <10 μm, although the diatoms >20 μm were abundant in the surface at NH-03 during the March 01 cruise. The biomass of flagellates <10 μm increased significantly ($p<0.05$, $t = 27.2$ $df = 2$)from NH-03 (3.26 ± 0.03 μgC/l) to NH-55 (9.26 ± 0.31 μgC/l) and dominated the low biomass stations. Cyanobacteria were never dominant and their biomass remained constant across the shelf.

The composition of the diatom community differed greatly between the April 2000 and the March 2001 cruises. During April 2000, the surface samples at NH-03 and NH-10 were dominated by *Chaetoceros*, with some *Skeletonema*, while in the subsurface chl maximum, *Skeletonema* dominated at NH-03 and unidentified single diatoms <10 μm dominated at NH-10 (Fig. 15). During the March 2001 cruise, the diatom community of NH-03 and NH-10 consisted of a mixture of *Chaetoceros*, *Thalassiosira*, and unidentified single diatoms >20μm in both the surface and subsurface chl maximum. However, at NH-20 and NH-55, the diatom community, in both the surface and subsurface chl maximum, was almost exclusively *Chaetoceros*.

Results. PartII- The Summer Upwelling Phytoplankton Bloom

Chl *a* in the Shelf, Slope and Offshore Regions. The relationship between total Chl *a* and the % Chl *a* >10 μm during summer and September cruises in the shelf, slope and offshore regions has a clear trend (Fig. 16). For total Chl *a* concentrations above 4 μg/l, the % Chl *a* >10 μm is always >50%. Low chl samples are dominated by phytoplankton <10 μm, while the high chl samples are dominated by phytoplankton >10 μm. The shelf region experiences a wide range of both total Chl *a* and % Chl *a* >10 μm, with a non-linear, though clearly defined relationship.

Variation of Inorganic Nutrients and Chl *a* with Temperature in the Shelf Region. Mean estimates of nitrate, phosphate, silicate, ammonium, total Chl *a* and % Chl *a* >10 μm from surface, 10 m and subsurface chl maximum samples collected from shelf stations during summer and September cruises of this study are listed in Table 9. The means are grouped by temperature ranges derived from the correlation of temperature with nitrate, phosphate and silicate.

Table 9: Mean and standard deviation of various parameters sampled during summer (August 1998, July 1999, 2000 and 2001) and September (1998, 1999, 2000) cruises over the shelf (<28 km from shore). Data are from all depths sampled for % Chl *a* >10 μm (surface, 10 m and subsurface chl maximum), and have been grouped by temperature based upon the regression between temperature and nitrate, phosphate and silicate concentrations.

	Nitrate (μM)	**Phosphate (μM)**	**Silicate (μM)**	**Ammonium (μM)**	**Tot Chl *a* (μg/l)**	**%Chl *a* >10μm**
<9ºC	27.6 (5.5)	2.3 (0.4)	40.6 (12.1)	0.53 (0.4)	2.9 (3.2)	69.5 (38.8)
9-12ºC	8.4 (5.8)	1.1 (0.6)	13.2 (7.7)	0.48 (0.3)	6.2 (5.4)	66.3 (27.7)
>12ºC	0.3 (0.5)	0.2 (0.2)	0.7 (1.3)	0.21 (0.2)	2.2 (0.9)	32.5 (30.4)

There is a distinct trend in the relationship between temperature and various inorganic nutrients for samples taken on these cruises (Fig. 17). The high r^2 values of the linear regressions at cooler temperatures suggest that nitrate, phosphate and silicate all decrease linearly with increasing temperature from about 8 to 12º C. Above about 12º C, the relationship is nearly flat, with nitrate and silicate depleted, and phosphate greatly reduced. Phosphate is usually not fully depleted. Ammonium tends to decrease with increasing temperature from 8 to 12º C, but the relationship is not statistically significant (Fig. 18).

Total Chl *a* and % Chl *a* >10 μm do not show a clear relationship with temperature (Fig. 19A). However, when the relationship between total Chl *a* and % Chl *a* >10 μm is plotted with respect to various temperatures, a pattern becomes evident (Fig. 19B). Plots of total Chl *a* and %Chl *a* >10 μm as a function of nitrate, phosphate and silicate all show clear patterns with respect to temperature (Figs. 20 and 21). Low temperature (<9º C) samples, which are high in nitrate, phosphate and silicate, have a high mean % Chl *a* >10 μm (69.5 ± 38.8 %), but total Chl *a* does not exceed 5 μg/l. One exception is a sample with high nitrate, phosphate and silicate, but for which the % Chl *a* >10 μm is 0.00 %. It should be noted that the total Chl *a* concentration of this sample is 0.39 μg/l, and therefore I would expect it to have a low % Chl *a* >10 μm. Between 9 and 12º C, total Chl *a* may reach as high as 14 μg/l, and mean % Chl *a* >10 μm is 66.3 ± 37.7 %. Above 12° C, when nitrate, phosphate and silicate are greatly reduced, total Chl *a* is <5 μg/l and % Chl *a* >10 μm ranges from 0 % to nearly 100% (Figs. 20 and 21; Table 9). One >12° C sample with depleted nitrate and phosphate is high in silicate (Fig. 21C). The across-shelf salinity distribution from the corresponding NEP-GLOBEC-LTOP cruise report indicates it is part of the Columbia River plume.

Ammonium and total Chl *a* concentrations both increase with increasing temperature from 9 to 12° C (Fig. 22A), although this relationship is quite variable and not statistically significant ($r^2 = 0.22$). Above 12° C, ammonium concentrations are <0.6 μM and Chl *a* concentrations are < 4 μg/l. The highest values of % Chl *a* >10 μm tend to correspond with the highest ammonium concentrations, which occur between 9 and 12° C (Fig. 22B).

Phytoplankton Taxa During the Summer Upwelling Phytoplankton Bloom. Distributions of the major phytoplankton taxa have been grouped by temperature in the same fashion as in the above analyses of total Chl *a,* % Chl *a* >10 μm and the inorganic nutrients (Fig. 23). As shown, total phytoplankton biomass increased, though not significantly ($p>0.5$, $t = 2.62$ $df = 2$), from 22.9 ± 9.6 μgC/l at 8° C to 136.9 ± 55.4 μgC/l at 11° C, and this increase in total biomass corresponds with an increase in diatom biomass, particularly diatoms between 10 and 20 μm (Fig. 23). In the <9° C samples, there is no significant difference ($p>0.05$, $t = 1.10$ $df = 2$) between the biomass of diatoms (77.6 ± 54.4 μgC/l) and the biomass

of flagellates (34.2 ± 12 μgC/l), but from about 9 to 11° C diatoms dominate (70.0 ± 30.2 % of total phytoplankton biomass).

Comparing the relative abundances of the specific groups of diatoms among the temperatures for which samples are available shows no clear relationship between dominance and temperature (Fig. 24). However, this plot illustrates that *Chaetoceros* and *Skeletonema* are responsible for the majority of both biomass and variability in the diatom community over the course of the bloom.

A plot of total Chl *a* versus temperature shows that fluctuations in total Chl *a* match those of Chl *a* >10 μm (Fig. 25A). Plotting together total Chl *a* and the abundance of *Skeletonema* and *Chaetoceros* versus temperature (Fig. 25B) shows that variability in the total Chl *a* signal matches changes in these two genera of diatoms closely. However, one peak in total Chl *a* (Fig. 25C at 8.7° C) is not correlated with a peak in diatom abundance, but instead with a peak in the abundance of flagellates >20 μm (dinoflagellates). For this sample, flagellate >20 μm biomass is only 8.7 ± 0.04 μgC/l, while the biomass of diatoms between 10 and 20 μm is 18.3 ± 1.8 μg C/l (Figure 25C). These results suggest that the majority of changes in phytoplankton stock over the course of the bloom can be attributed to changes in the diatom assemblage, particularly among *Chaetoceros* and *Skeletonema.* Dinoflagellates also contribute to the phytoplankton standing stock, but not as much as diatoms.

Discussion - Seasonal and Across-Shelf Environmental Variability

"How do phytoplankton biomass, size structure and the diversity of the phytoplankton community vary seasonally and with distance from shore off the Oregon coast?"

From the results of this study, it is apparent that phytoplankton biomass, and community composition do vary across the shelf and seasonally, and these across-shelf and seasonal patterns recur from year-to-year. During every season, flagellates <10 μm dominate at the offshore stations (NH-20 and NH-55), and their offshore abundance persists shoreward across the shelf. Changes in the diatoms, particularly diatoms of the genera *Chaetoceros* and *Skeletonema,* account for most of the change in phytoplankton biomass, as well as in phytoplankton community composition. These two genera, along with other chain formers such as *Thalassiosira*, frequently dominate over the shelf. In the offshore region, diatoms are present during every season, even the winter, but their biomass is almost always low (<1 μg C/l). Cyanobacteria never account for more than approximately 10% of phytoplankton biomass in any given sample, even though they may be very abundant numerically.

The summer (July and August) is marked by the strongest and most consistent upwelling of any season. Consequently, nearshore (<28 km from shore) integrated Chl *a* concentrations are higher then and persist farther offshore. Associated with high integrated Chl *a* are high values of % Chl *a* >10 μm, indicating that net-phytoplankton account for the majority of phytoplankton stock over the shelf. Taxonomic analysis of these samples found again that, *Chaetoceros* and *Skeletonema* accounted for the majority of phytoplankton biomass over the shelf during the July 2000 and 2001 cruises.

Beyond the shelf (> 28km from shore), integrated Chl *a* and % Chl *a* >10 μm decrease substantially. Taxonomic analysis shows that nanoflagellates <10 μm account for the majority of phytoplankton biomass at these low chl stations. It is the almost complete absence of the chain-forming diatoms that accounts for the reduced standing stock and typical offshore phytoplankton community composition. These findings agree with previous work off the Oregon coast by Kokkinakis and Wheeler (1988), who found during summer that net-phytoplankton, particularly chain-forming diatoms, dominated in high nitrate regions, while nanophytoplankton dominated in low nitrate regions. Both studies support previous work (Malone, 1981; Chisholm; 1989; Booth, 1988; Booth, 1993) that suggests that high nutrient regions tend to be dominated by net-phytoplankton, particularly chain-forming diatoms, while offshore oligotrophic regions tend to be dominated by nanophytoplankton.

September and spring are similar to each other, as well as to summer, in their distribution of integrated Chl *a* and % Chl *a* >10 μm. However, integrated Chl *a* is not so high nearshore in either September or spring as it is during July and August, and consequently the across-shelf difference is much less. September's reduced phytoplankton biomass relative to the summer peak may be due to decreased upwelling, though this is not always the case. For example, the upwelling index during the September 1999 cruise was greater than that during the July 1999 cruise. The difference in phytoplankton biomass between the spring and summer could also be due to differences in upwelling between the two seasons. During the summer, multiple upwelling events lasting from two to 10 days consistently provide nutrients for extensive phytoplankton blooms (Small and Menzies, 1981). The spring, however, does not experience as many upwelling events (Huyer, 1983), and therefore phytoplankton stock may not be able to reach the same concentrations as it does during the summer.

Unlike the April and July 2000 and the March 2001 cruises, in which diatoms dominated nearshore stations, these same stations, during the September 2000, cruise were dominated by flagellates <20 μm, and diatoms were few. The shift from a diatom-dominated community during the July 2001 cruise to a flagellate-dominated community during the September cruise may be the result of nutrient depletion after the summer blooms. The surface nitrate concentrations at NH-10, 20 and 50 were all undetectable. However, surface nitrate at NH-03 was high enough (12.6 μM) to facilitate diatom growth. Hood et al. (1992) also found that flagellates, not diatoms dominated the nearshore phytoplankton community during September, indicating a consistent difference between summer and September phytoplankton communities.

Winter (November, January and February) differs from the other seasons in its across-shelf distribution of both integrated Chl *a* and % Chl *a* >10 μm. Integrated Chl *a* and % Chl *a* >10 μm do not change across the shelf and are consistently low. This low phytoplankton standing stock is probably due to the strong downwelling and deeper mixing (50 – 80m, see Huyer, 1983) that characterize those months. However, the January 2001 cruise suggests that, even though integrated Chl *a* may not change across the shelf, the phytoplankton community composition does. Diatoms still dominated among the nearshore phytoplankton, with the genera *Chaetoceros, Skeletonema,* and *Thalassiosira* most abundant. Surf diatom productivity is greatest during the winter months and the genus *Chaetoceros* is one of the dominant genera in the surf along the Oregon coast (Lewin et al., 1989). The *Chaetoceros* I found in this study may be remnants of surf diatom populations, suggesting that waters right at the beach may provide a seed stock of *Chaetoceros* to nearshore waters during the winter.

Discussion - The Summer Upwelling Phytoplankton Bloom

"How do inorganic nutrient concentrations, temperature, phytoplankton biomass, size fractionation and taxonomic community diversity change over the course of a summer phytoplankton bloom off the Oregon coast?"

Looking just at shelf samples (NH-03 to NH-15), nitrate and silicate all decrease with increasing temperature from 8 to 12° C, while above 12° C the relationship is nearly flat. Two of the surface (< 3 m) samples used in this study have temperatures ≤9° C, indicating they are from recently upwelled water. Nutrient concentrations of these samples are 51.90 and 31.62 μM for silicate, 31.20 and 22.3 μM for nitrate and 2.66 and 1.97 μM for phosphate. Decrease of inorganic nutrients from these levels is undoubtedly linked to the progression of phytoplankton blooms. As blooms progress, nutrients are depleted by the phytoplankton, and persistent residence of water near the surface increases its temperature. The important findings here are how consistent this trend is, that it is evident in phosphate, nitrate, and silicate, and that Chl *a* and % Chl *a* >10 μm also vary with nutrients and temperature in a consistent fashion.

Total Chl *a* concentrations of samples ≤9° C, are relatively low (2.9 ± 3.2 μg/l), but the mean % Chl *a* >10 μm of these samples is high (69.5 ± 38.8 %), indicating they are dominated by net-phytoplankton, in particular chain-forming diatoms. The mean % Chl *a* >10 μm does not reach 100%, because nanoflagellates are still present in these samples, even though their biomass is very small relative to diatom biomass (Fig. 23). At temperatures above 12° C, nutrients have been depleted, or are greatly reduced, Chl *a* concentrations have decreased and % Chl *a* >10μm shifts down as these low nutrient conditions favor smaller cells (Malone, 1980; Chisholm, 1992; Grover, 1989).

The highest total Chl *a* concentrations (>5 μg/l) are only found at temperatures between 9 and 12° C, and the high mean % Chl *a* >10 μm (66.3 ± 27.7 %) of these samples indicates they are net-phytoplankton dominated. However, lower Chl *a* concentrations (<2 μg/l) and lower % Chl *a* >10 μm (<50 %) also occur between these temperatures (Fig. 19). Because these data are from multiple cruises, over several years, it is possible that this variation is due to differences between the cruises. For example, the three highest total Chl *a* concentrations are all from the August 1998 cruise. This highlights the limitation of using multiple cruises, during parts of different blooms, to characterize the typical stages of phytoplankton blooms.

Ammonium increases, though not significantly, from 8 to 12° C, and the highest ammonium concentrations are found in the 9 to 12°C samples, corresponding to the peaks of blooms sampled during multiple cruises. High phytoplankton standing stock may lead to increased ammonium concentrations through a several different mechanisms: direct release of ammonium by phytoplankton into the water, loss of ammonium from phytoplankton being grazed and release of ammonium by grazers. Above 12° C, ammonium, along with the other nutrients, is almost entirely depleted. Morris et al. (1985) found similar results in the coastal waters of Scotland. Early in the spring bloom, nitrate was high, then decreased as ammonium increased, but eventually both were depleted

Our attempt to track the major taxonomic changes occurring through the different parts of upwelling cycles showed that during the phytoplankton peak (at 9-12° C) most of the stock was dominated by 10-20 μm diatoms, in particular, diatoms of the genera *Chaetoceros* and *Skeletonema.* These are the most common genera of diatoms found nearshore year-round in this system, as well as in other temperate and upwelling ecosystems (Morris et al, 1985; Marrassé et al., 1989; Pitcher et al., 1993; and Ragueneau et al., 1994). The strong relationship between the biomass of these genera and total Chl *a* indicates that their abundance determines, to a great extent, the Chl *a* concentrations in this system. However, dinoflagellates (>20 μm) can also contribute infrequently or briefly. Because these taxonomic data are from three separate cruises and do not represent a complete time-series of any particular bloom progression, they do not show whether this variability in phytoplankton community composition results from available seed stock prior to the bloom or is due to advection of cells into the study area, possibly from the surf zone as mentioned earlier or possibly from sources upstream either alongshore or offshore. *Chaetoceros* (Hasle, 1996), and possibly *Skeletonema,* also form spores that rest in sediments and may be another source of bloom-initiating cells.

The results of this study are similar to those of Pitcher et al. (1993) and Ragueneau et al., (1994). Pitcher et al. (1993) found, in the Benguela upwelling system, that early in periods of upwelling-induced blooms at temperatures of 9.9-11° C and with high nutrients (nitrate: 12.6-26.6 μM), Chl *a* concentrations followed a similar trend as in this study. Initial concentrations were between 0.01 – 0.31 μg/l, reached maximum concentrations of 10 – 20 μg/l, and then decreased to <3 μg/l after the peak. Also as in this study, the changes in phytoplankton biomass were almost solely due to changes in the abundance of *Chaetoceros*, *Thalassiosira* and *Skeletonema*. Unfortunately, their study was performed in a microcosm, and changes in the composition of the natural phytoplankton community were not monitored. The *in situ* study by Ragueneau et al. (1994) found that the most abundant groups of diatoms over the course of the spring bloom in the Bay of Brest were *Skeletonema*, *Thalassiosira*, *Rhizosolenia*, and *Chaetoceros*.

Similarly, Morris et al. (1985) found that *Skeletonema* dominated during blooms in their *in situ* experimental studies in Scotland, but they also found high concentrations of *Nitzschia,* which were never abundant in this study.

Literature Cited

Austin, J. A. and J. A. Barth. In Press. Variation in the position of the upwelling front on the Oregon Shelf. Journal of Geophysical Review.

Barber, R. T. and R. L. Smith. 1981. Coastal upwelling ecosystems. In: A. R. Longhurst (ed) *Analysis of Marine Ecosystems*. Academic Press, London p. 31-68.

Booth, B. C., Lewin, J. and J. R. Postel. 1993. Temporal variation in the structure of autotrophic and heterotrophic communities in the subarctic Pacific. Prog. Oceanog. 32: 57-99.

Booth, B. C. 1993. Estimating cell concentration and biomass of autotrophic plankton using microscopy In: P.F. Kemp, B.F. Sherr, E.B. Sherr & J.J.Cole (eds.) *Handbook of Methods in Aquatic Microbial Ecology*. Lewis Publishers Boca Raton, FL p. 199-206.

Booth, B. C. 1988. Size clases and major taxonomic groups of phytoplankton at two locations in the subarctic Pacific Ocean in May and August, 1984*. Marine Biology. 97: 275-286.

Chisholm, S. W. (1992). Phytoplankton size. In: P.G. Falkowski & A.D Woodhead (eds.) *Primary Productivity and Biogeochemical Cycles in the Sea*. New York: Plenum Press. p. 213 – 238.

Corwith, H. L. 2000. El Niño related variations in nutrient and chlorophyll distributions off Oregon and northern California. M.S. thesis, Oregon State University, 109pp.

Corwith, H. L. and P. A. Wheeler. In Press. El Niño related variations in nutrient and chlorophyll distributions off Oregon. Progress in Oceanography.

Fleischbein, J. A., Hill, J. K., Huyer, A., Smith, R. L., and P. A. Wheeler. 1999. Hydrographic data from GLOBEC long-term observation program off Oregon, 1997 and 1998. Data Report 172, Ref. 99-1. Oregon State University, 288pp.

Gordon, L. I., Jennings, J. C., Ross, A. R., and J. M. Krest. (1995). A suggested protocol for continuous flow automated analysis of seawater nutrients (phosphate, Nitrate, nitrite, and silicic acid) in *WOCE Hydrographic Program and the Joint Global Ocean Fluxes Study*. Oregon State University Technical Report. 93-1 (rev).

Grover, J. P. 1989. Influence of cell shape and size on algal competitive ability. Journal of Phycology. 25: 402-405.

Hasle, G. R. and E. E. Syvertsen. 1996. Marine diatoms. In: Tomas, C. R. (ed.) Identifying marine diatoms and dinoflagellates. Academic Press, Inc., San Diego, p. 5-385.

Hickey, B. M. 1989. Ch. 2. Patterns and processes of circulation over the Washington continental shelf and slope. In Landry, M.R. and B.M. Hickey (eds.) *Coastal Oceanography of Washington and Oregon.* Elsevier Oceanography Series, 47, New York, p. 41-109

Hill, J. K. and P. A. Wheeler. 2002. Organic carbon and nitrogen in the northern California Current system: comparison of offshore, river plume, and coastally upwelled waters. Progress in Oceanography.

Hood, R. R., S. Neuer and T. J. Cowles. 1992. Autotrophic production, biomass and species composition at two stations across an upwelling front. Mar. Ecol. Prog. Ser. 83: 221-232.

Huyer, A. 1983. Coastal upwelling in the California Current system. Progress in Oceanography 12: 259-284.

Kokkinakis, S. A. and P. A. Wheeler. 1988. Uptake of ammonium and urea in the northeast Pacific: comparison between netplankton and nanoplankton. Marine Ecology Progress Series. 43: 113-124.

Lewin, J., C. T. Schaefer, and D. F. Winter. 1989. Ch 12. Surf-zone ecology and dynamics. In Landry, M. R. and B. M. Hickey (eds.) *Coastal Oceanography of Washington and Oregon*. Elsevier Oceanography Series, 47, New York, p. 567-600.

Malone, T.C. 1980. Size fractionated primary productivity of marine phytoplankton in P.G. Falkowski *Primary Productivity in the Sea*. Plenum, NewYork, p. 301-318.

Marrasé, C., C. M. Duarte and D. Vaqué. 1989. Succession patterns of phytoplankton blooms: directionality and influence of algal cell size. Marine Biology. 102: 43-48.

Morris, R.J., M. J. McCartney, I. R. Joint and G. A. Robison. 1985. Further studies of a spring phytoplankton bloom in an enclosed experimental ecosystem. J. Exp. Mar. Biol. Ecol. 86: 151-170.

Parsons, T. R., Y. Maita, and C. M. Lalli. 1984. A manual of chemical and biological methods for seawater analysis. Pergamon Press, Oxford, 173pp.

Peterson, W. T., J. E. Keister, and L. R. Feinberg. 2002. The effects of the 1997-99 El Niño/La Niña events on the hydrography and zooplankton of the central Oregon Coast. Progress in Oceanography.

Peterson, W. T., C. B. Miller and A. Hutchinson. 1979. Zonation and maintenance of copepod populations in the Oregon upwelling zone. Deep-Sea Research. 26A: 467-494.

Ragueneau, O., E. D Varela, P. Trégeuer, B. Quéguiner, and Y.D. Amo. 1994. Phytoplankton dynamics in relation to the biogeochemical cycle of silicon in a coastal ecosystem of western Europe. Mar. Ecol. Prog. Ser. 106: 157-172.

Pitcher, G. C., J. J. Bolton, P. C. Brown and L. Hutchings. 1993. The development of phytoplankton blooms in upwelled waters of the southern Benguela upwelling system as determined by microcosm experiments. J. Exp. Mar. Biol. Ecol. 165: 171-189.

Riley, G. A. 1956. Oceanography of Long Island Sound, 1952-1954. 2. Physical Oceanography, *Bull. Bingham Oceanogr. Collection*, 15, 15-46.

Sherr, E. B., D. A. Caron and B. F. Sherr. 1993. Staining of heterotrophic protests for visualization via epifluorescence microscopy. In P.F. Kemp, B.F. Sherr, E.B. Sherr & J.J.Cole (eds.) *Handbook of Methods in Aquatic Microbial Ecology* Lewis Publishers, Boca Raton, FL, p. 213-228.

Small, L. F., and D. W. Menzies. 1981. Patterns of primary productivity and biomass in a coastal upwelling region. Deep-Sea Research. 28A:123-149.

Small, L.F. and H. Curl. 1968. The relative contribution of particulate chlorophyll and river tripton to the extinction of light off the coast of Oregon. Limnology and Oceanography. 13: 84-91.

Smith, R.L., A. Huyer, and J. Fleischbein. 2001. The coastal ocean off Oregon from 1961 to 2000: is there evidence of climate change or only of Los Niños? Progress in Oceanography.

Strathmann, R. R. 1967. Estimating the organic carbon content of phytoplankton from cell volume or plasma volume. Limnology and Oceanography. 12: 411-418.

Strom, S.L., M. A. Brainard, J.L. Holmes and M.B. Olson. 2001. Phytoplankton blooms are strongly impacted by microzooplankton grazing in coastal North Pacific waters. Marine Biology. 138: 355-368.

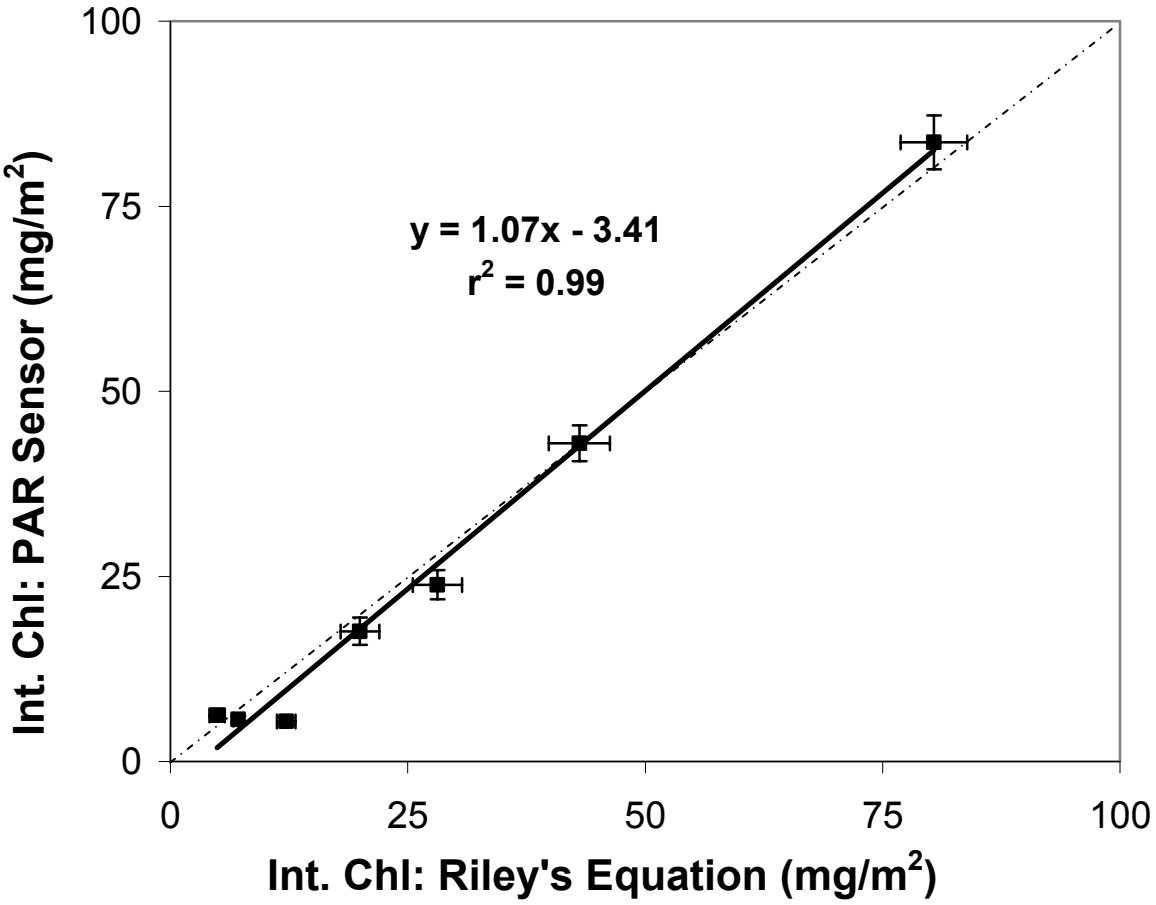

Figure 1: Integrated Chl *a* values calculated using PAR sensor estimates of euphotic zone depth against integrated Chl *a* values calculated from estimates of euphotic zone depths using Riley's equation. Data are from the September 2000 and January 2001 cruises. The dashed line indicates a 1:1 ratio. Error bars represent standard deviations obtained from maximum and minimum estimates of integrated Chl *a* based upon the highest and lowest values of the two total chl samples. The equation represents the best fit linear estimation of the data.

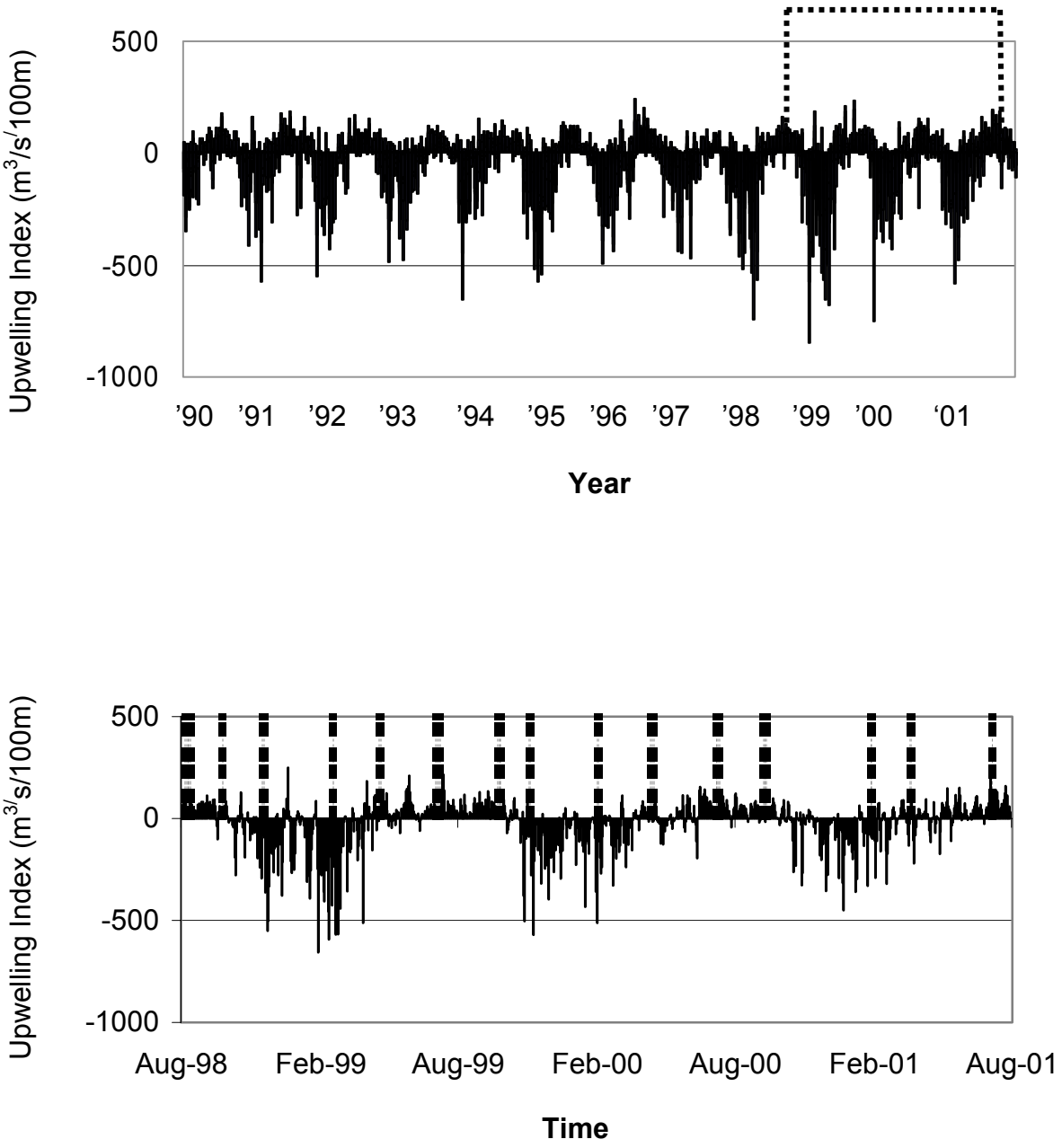

Figure 2. Daily average upwelling index at 45ºN 125ºW in units of Ekman transport with positive values indicating offshore transport. Estimates were calculated from Ekman's theory of mass transport using daily averaged windstress divided by the Coriolis force. Data were downloaded from www.pfeg.noaa.gov. A. Upwelling index values for January 1990 to October 2001. The dashed box indicates the period of this study. B. Upwelling index over the period of the study. Dashed lines indicate dates of cruises in the study.

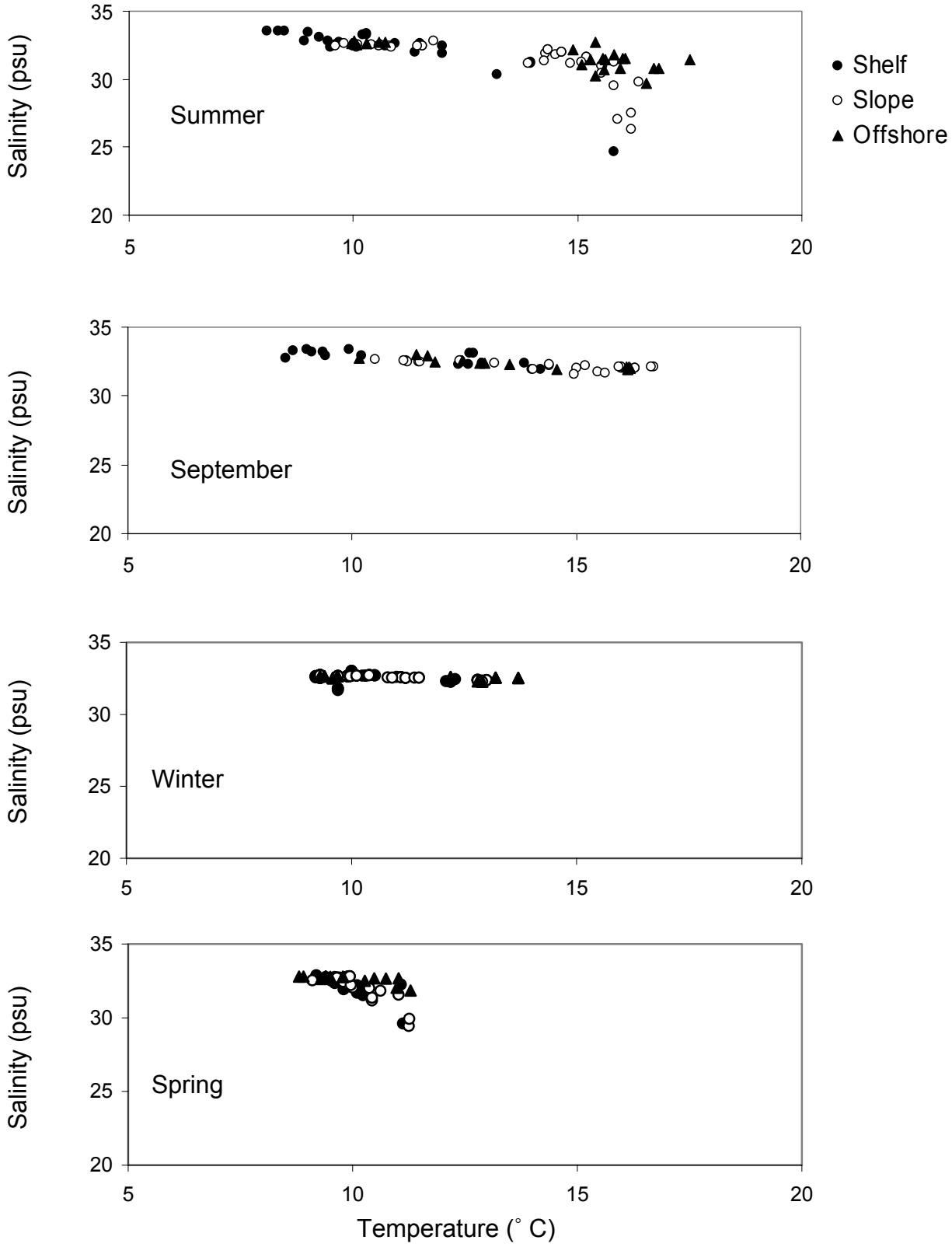

Figure 3: Surface temperature and salinities for the various seasons, grouped according to the shelf, slope and offshore stations.

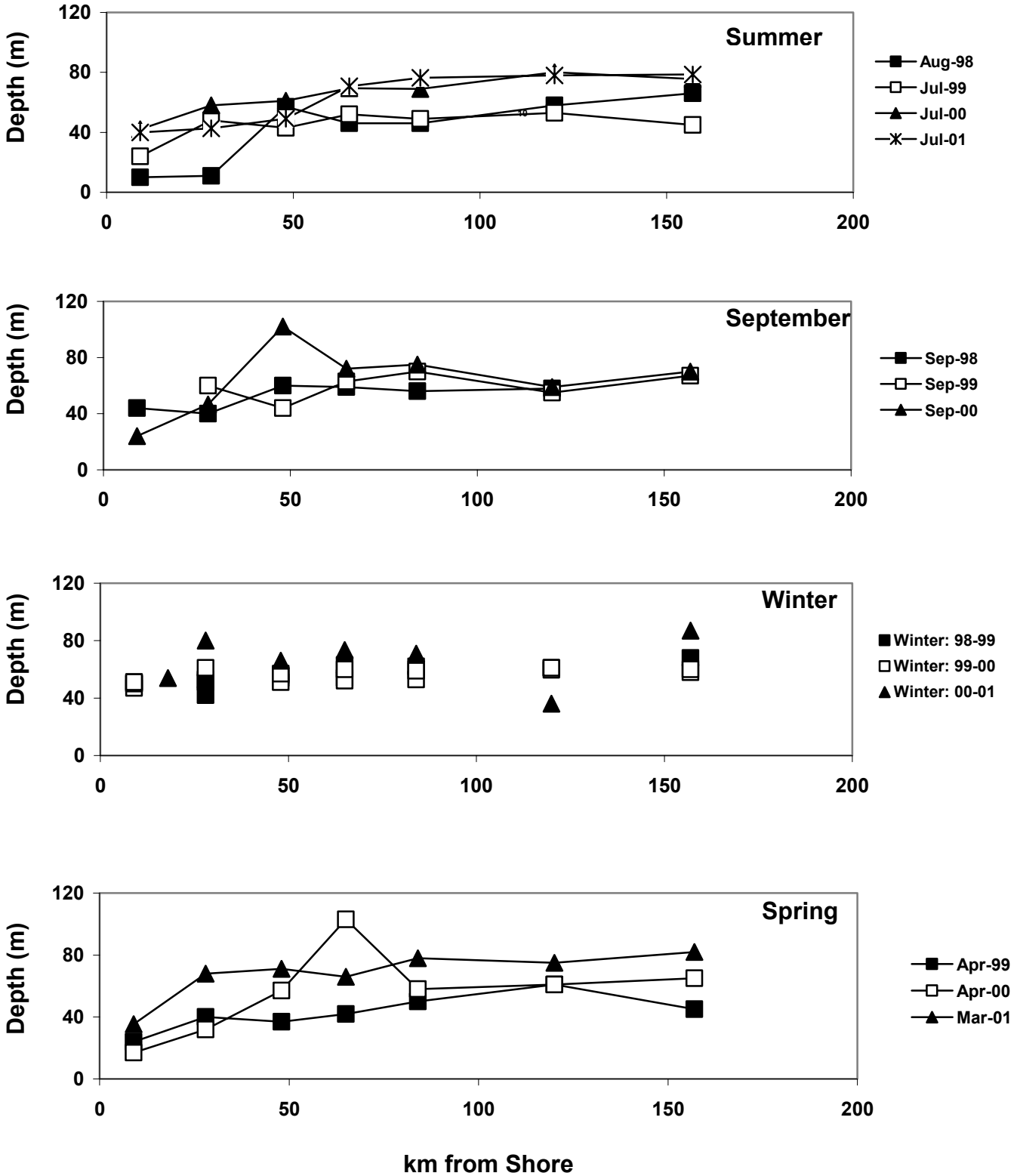

Figure 4: Euphotic zone depth as a function of distance from shore, grouped by season. The separate lines represent the various cruises during that season. Lines are omitted from "winter" because multiple samplings at each station make lines difficult to interpret

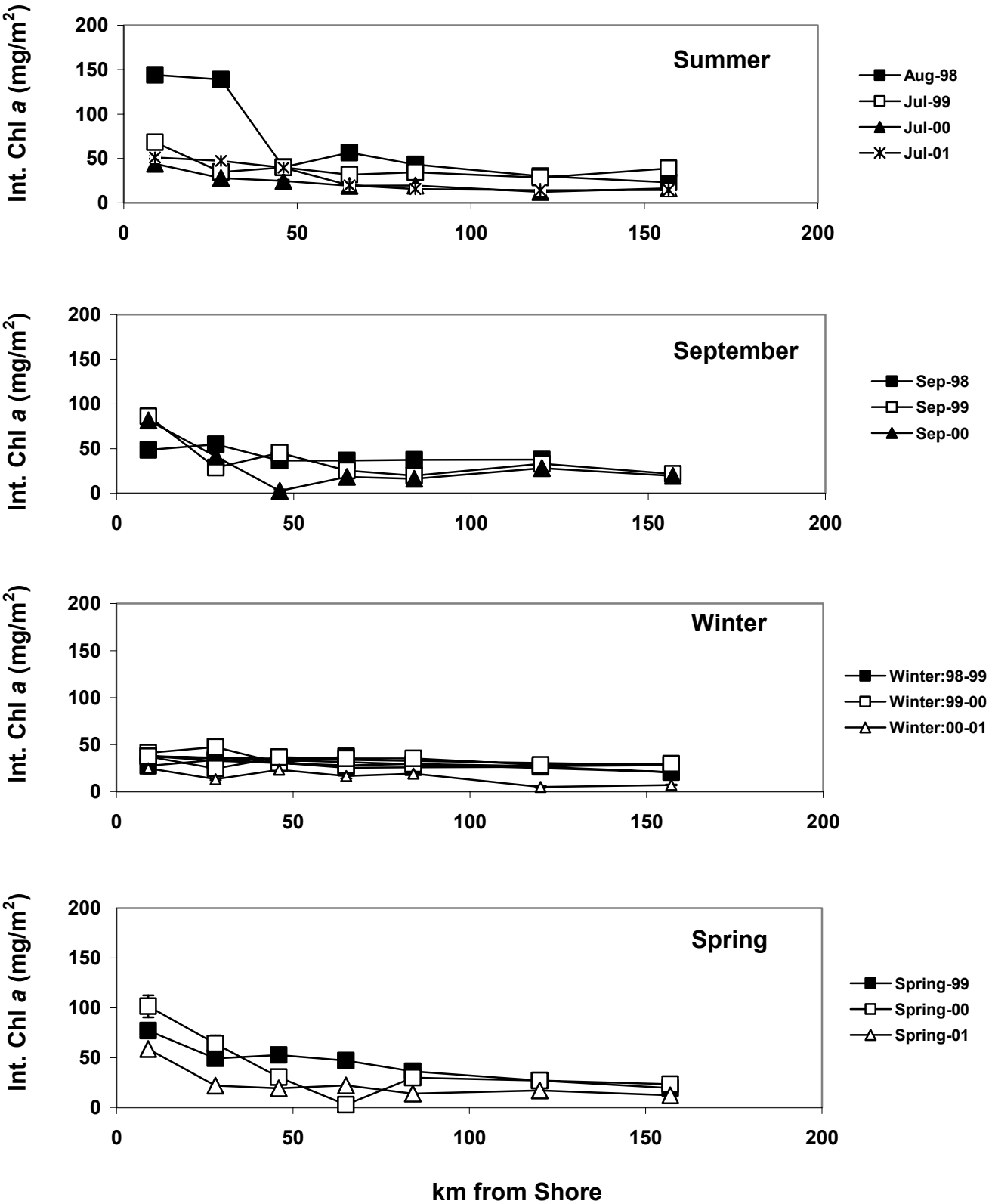

Figure 5: Integrated Chl *a* as a function of distance from shore, grouped by season. The separate lines represent the various cruises during that season. Error bars represent the standard deviation between the maximum and minimum estimates.

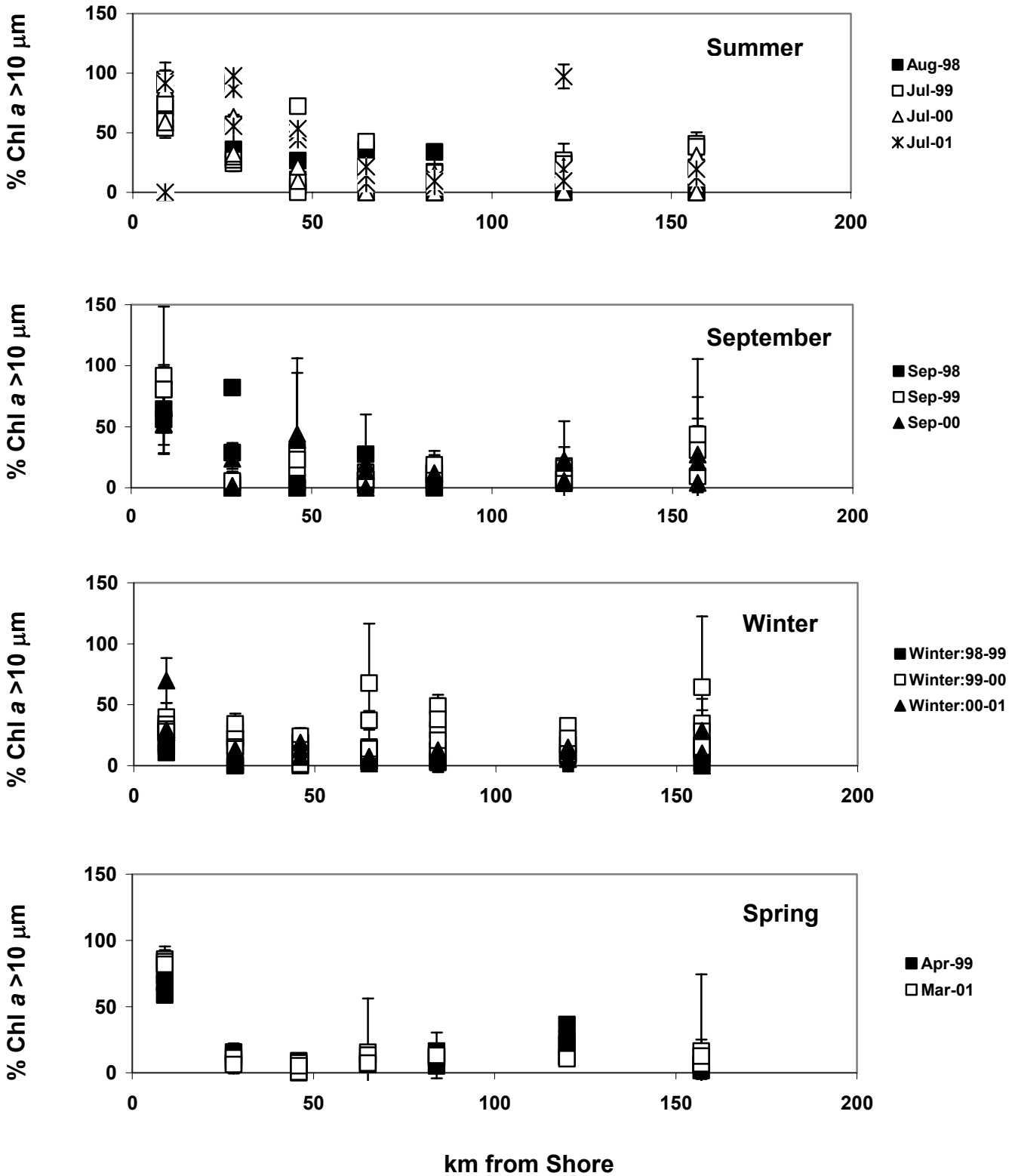

Figure 6: Percent Chl *a* >10 µm as a function of distance from shore, grouped by season. The different colors distinguish the different cruises during that season. The multiple points at a given distance from shore represent different depths sampled.

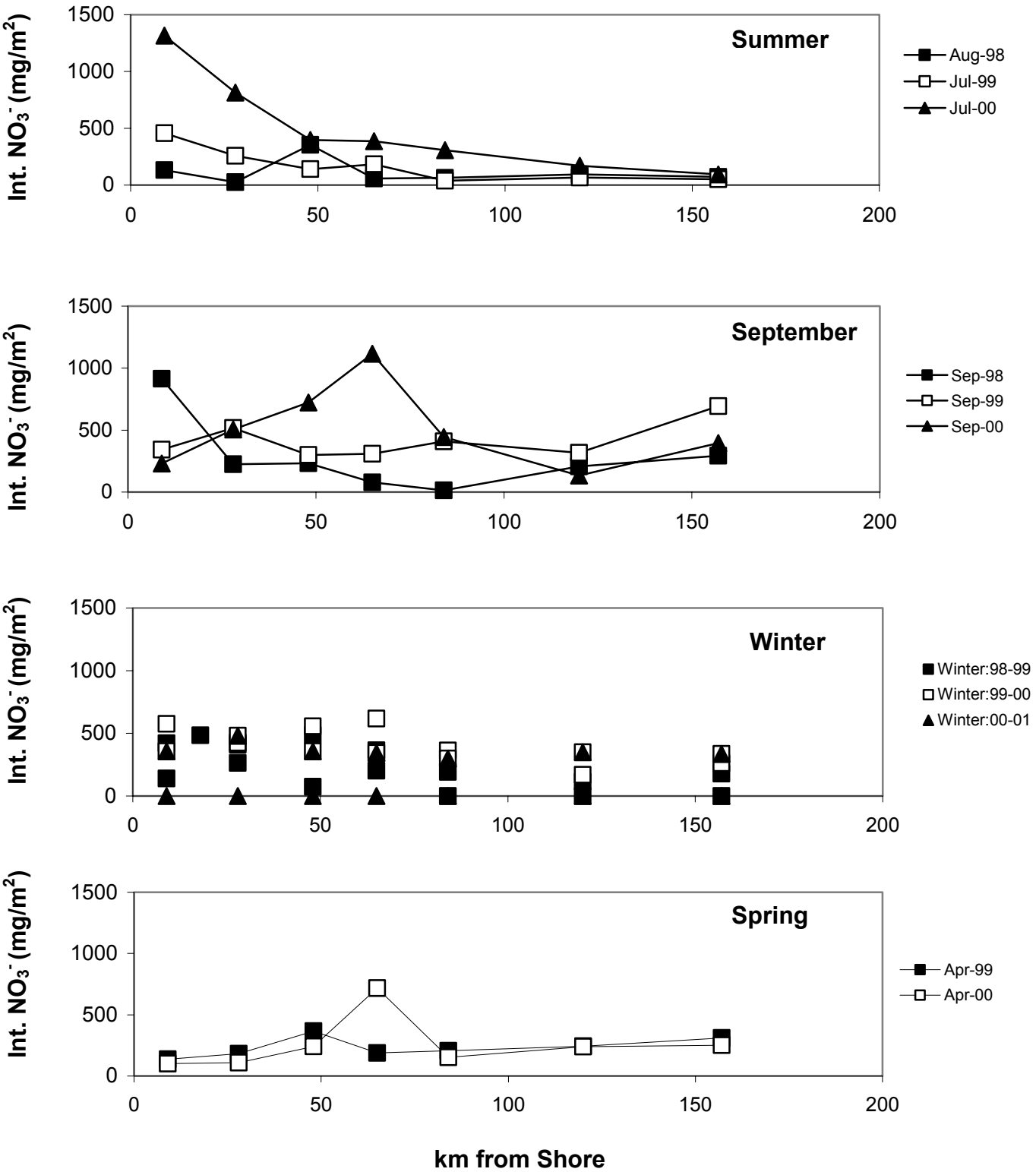

Figure 7: Integrated nitrate, integrated to the depth of the euphotic zone as a function of distance from shore, grouped by season. The separate lines represent the various cruises during that season.

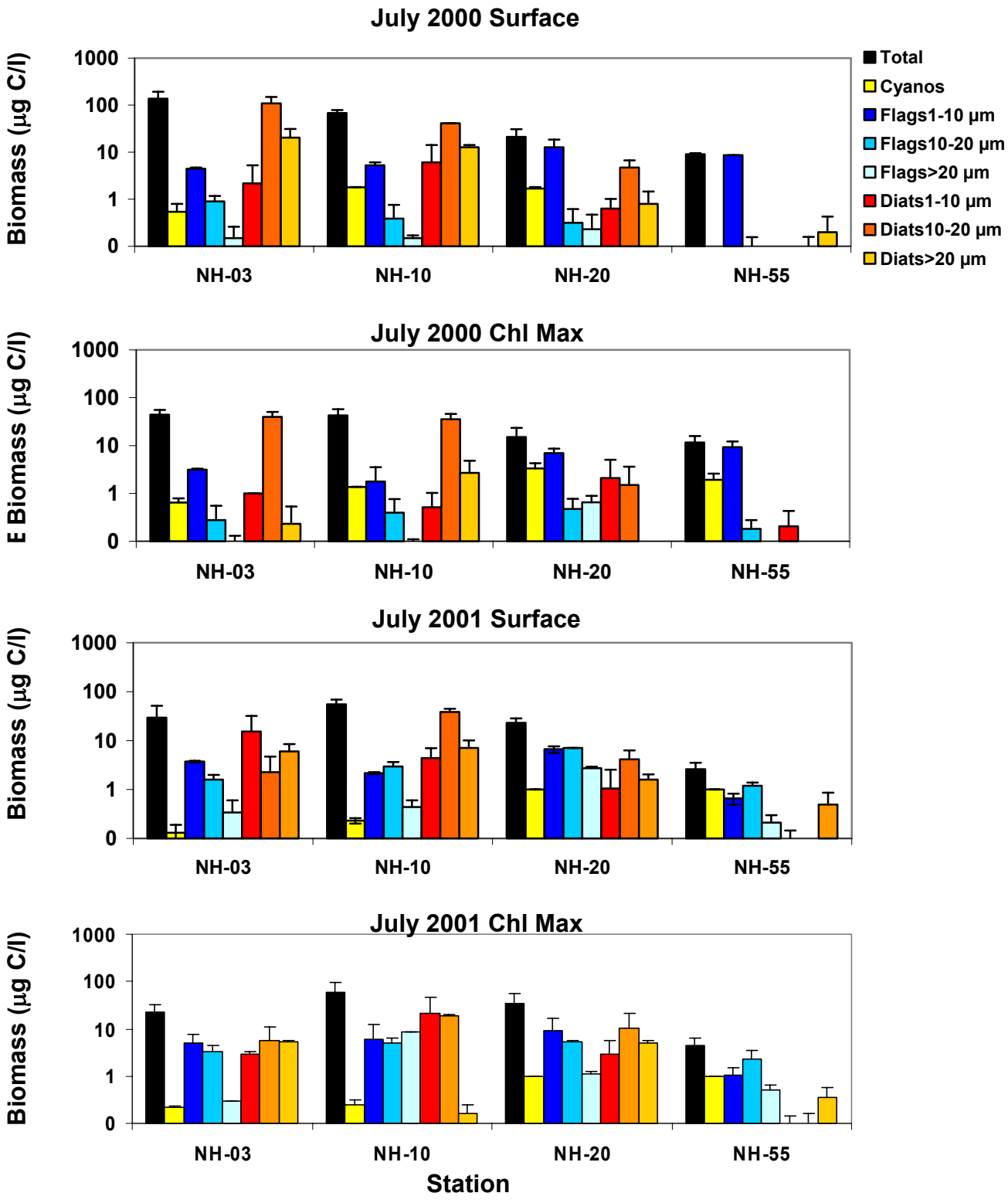

Figure 8: July 2000 and 2001 distribution of total phytoplankton biomass, cyanobacteria biomass, and the biomass of various sizes of flagellates and diatoms in both the surface and subsurface chl maxima. Error bars represent standard deviations between duplicate samples.

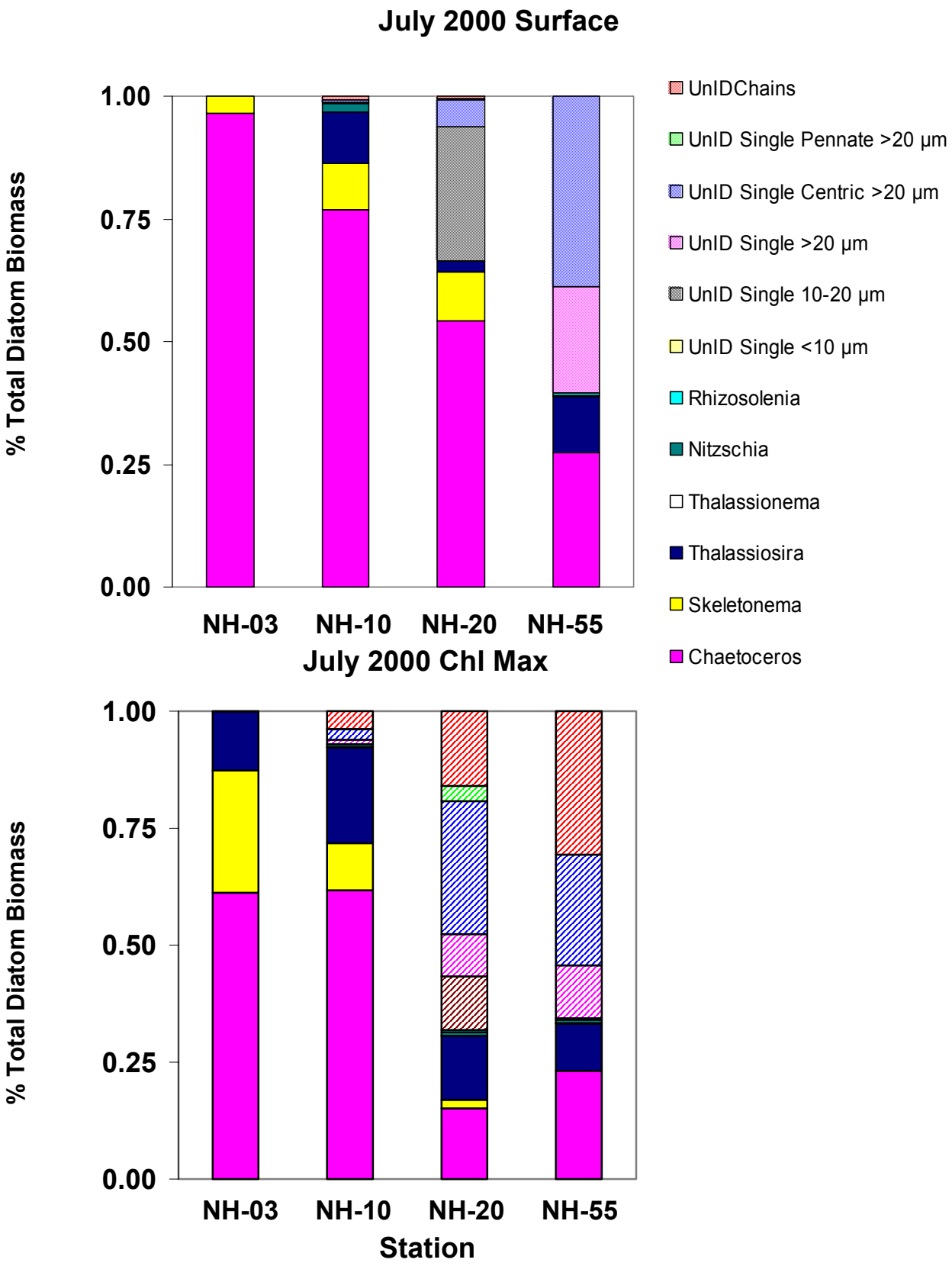

Figure 9: July 2000 and 2001 across shelf distribution of major groups of diatoms in the surface and subsurface chl maxima as a function of total diatom biomass.

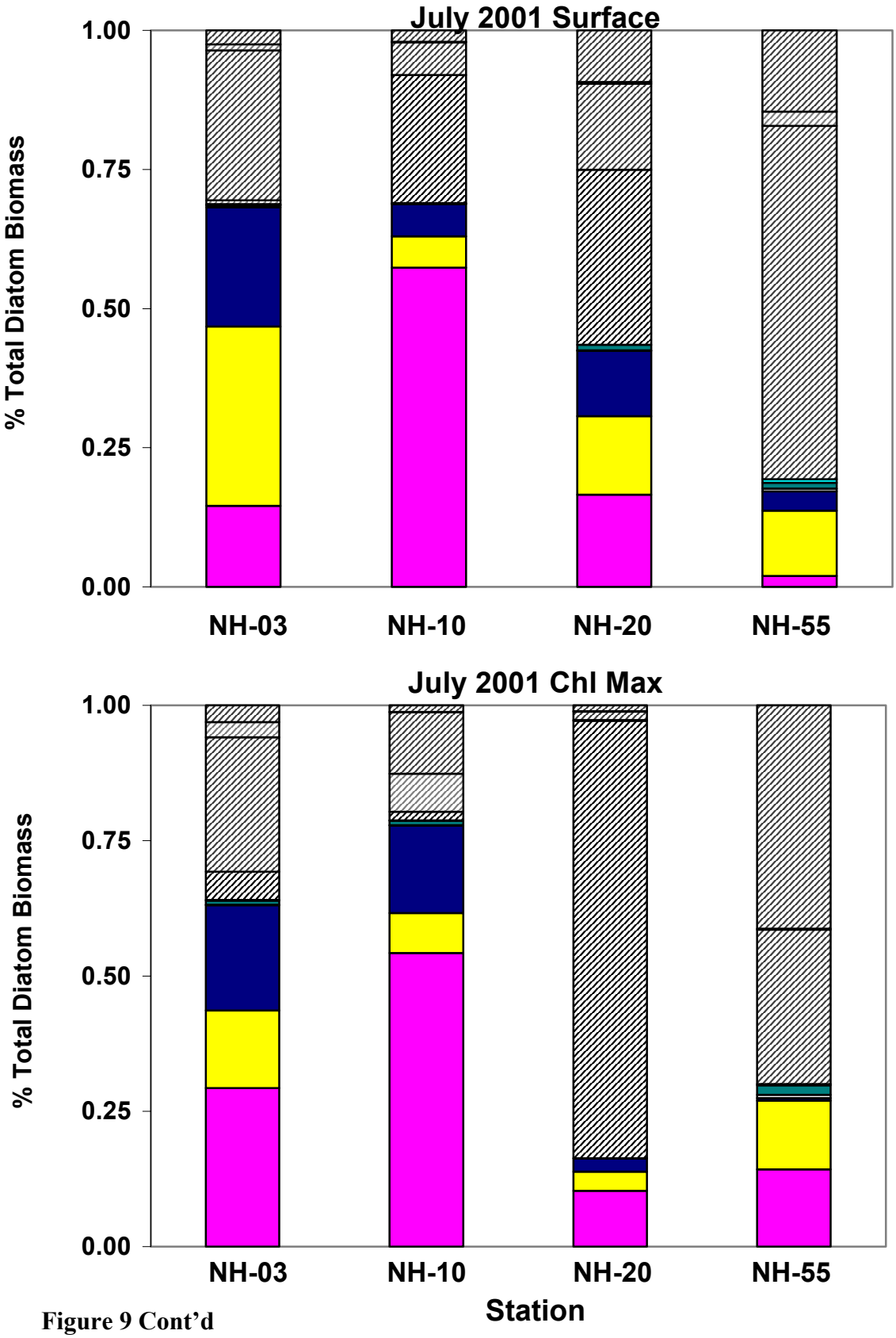

Figure 9 Cont'd

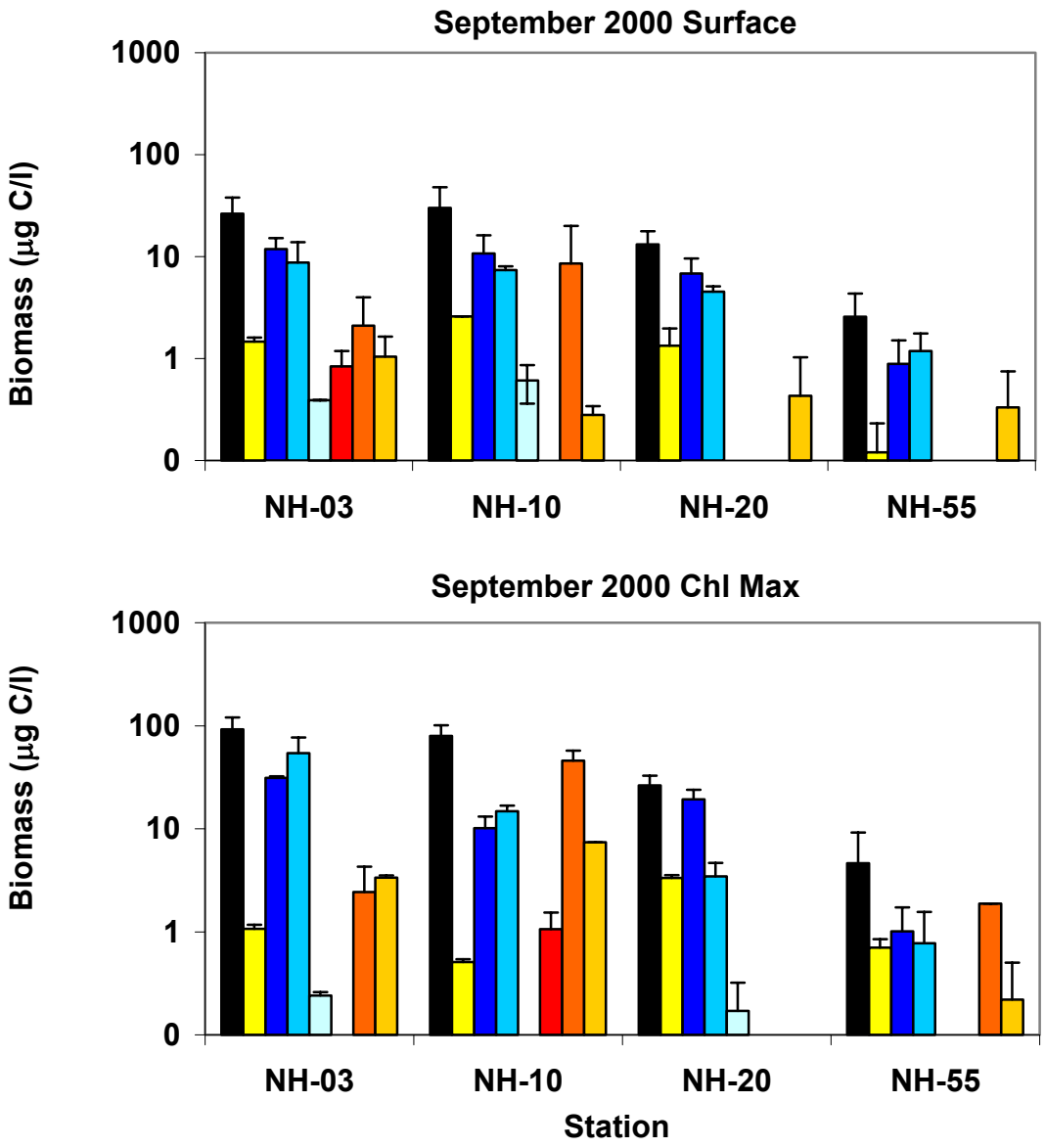

Figure 10: September 2000 distribution of total phytoplankton biomass, cyanobacteria biomass, and the biomass of various sizes of flagellates and diatoms in both the surface and subsurface chl maxima. Error bars represent standard deviations between duplicate samples. Refer to Figure 8 for legend.

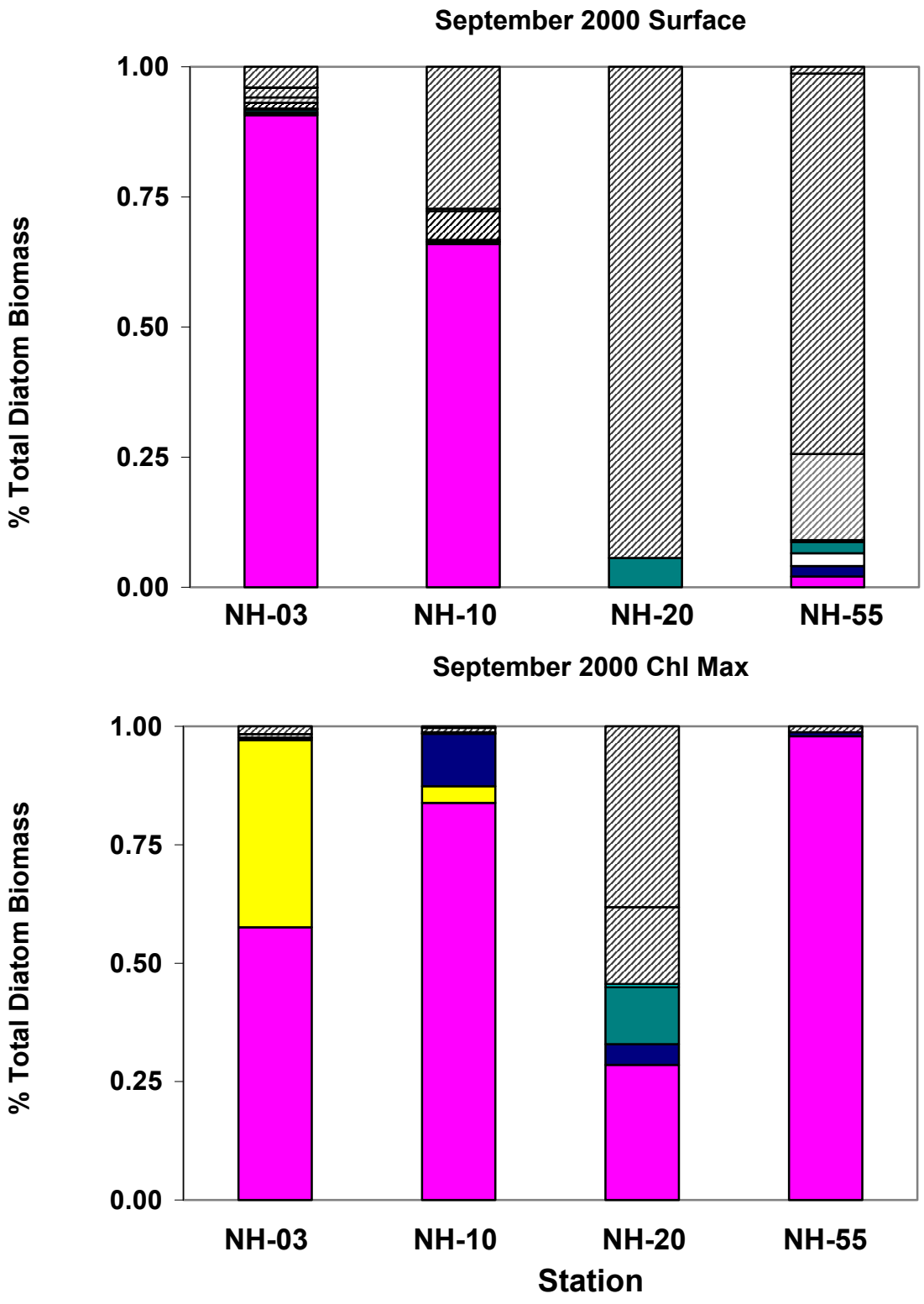

Figure 11: September 2000 across shelf distribution of major groups of diatoms in the surface and subsurface chl maxima as a function of total diatom biomass. Refer to Figure 9 for legend.

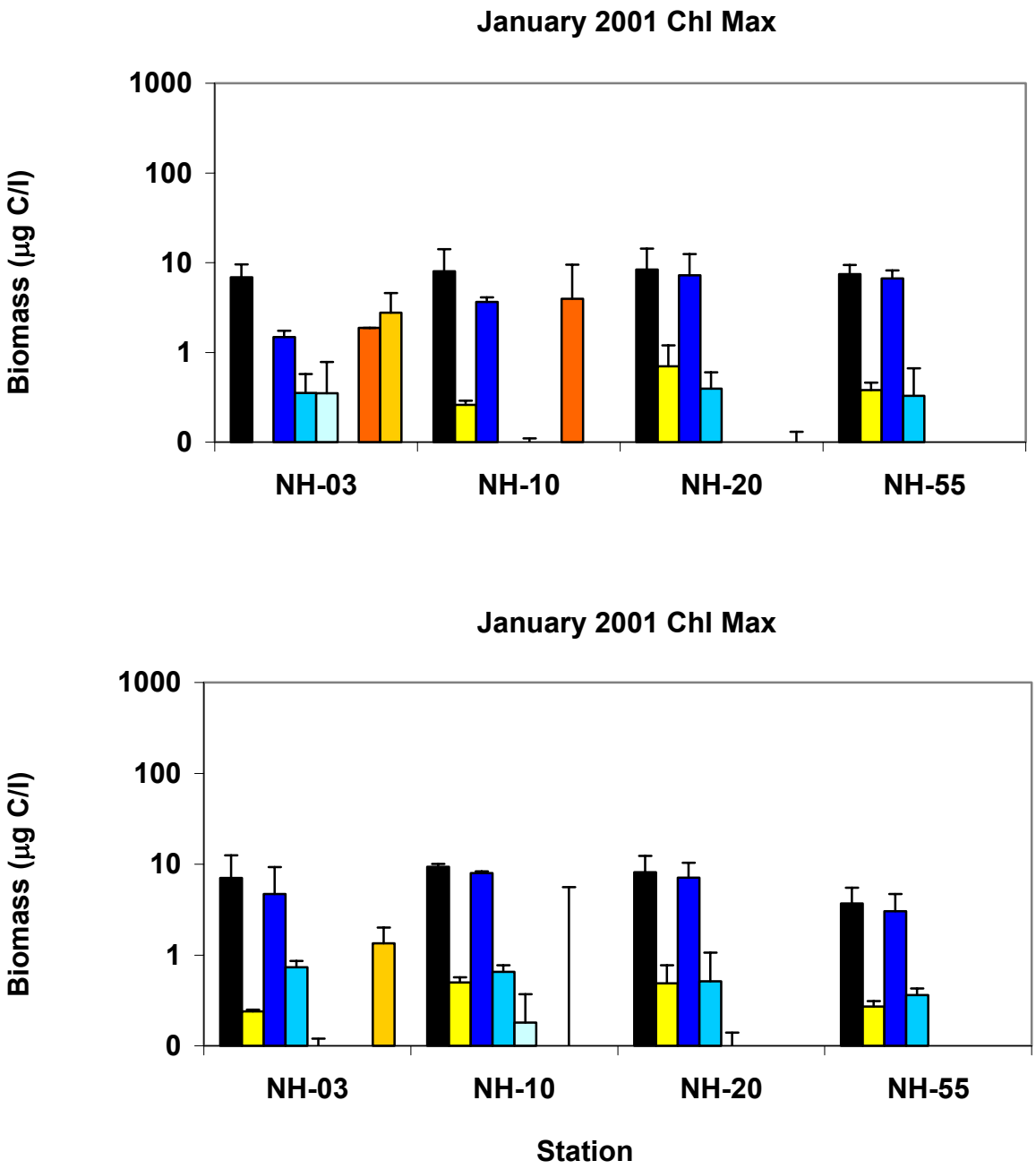

Figure 12: Winter (January 2001) distribution of total phytoplankton biomass, cyanobacteria biomass, and the biomass of various sizes of flagellates and diatoms in both the surface and subsurface chl maxima. Error bars represent standard deviations between duplicate samples. Refer to Figure 8 for legend.

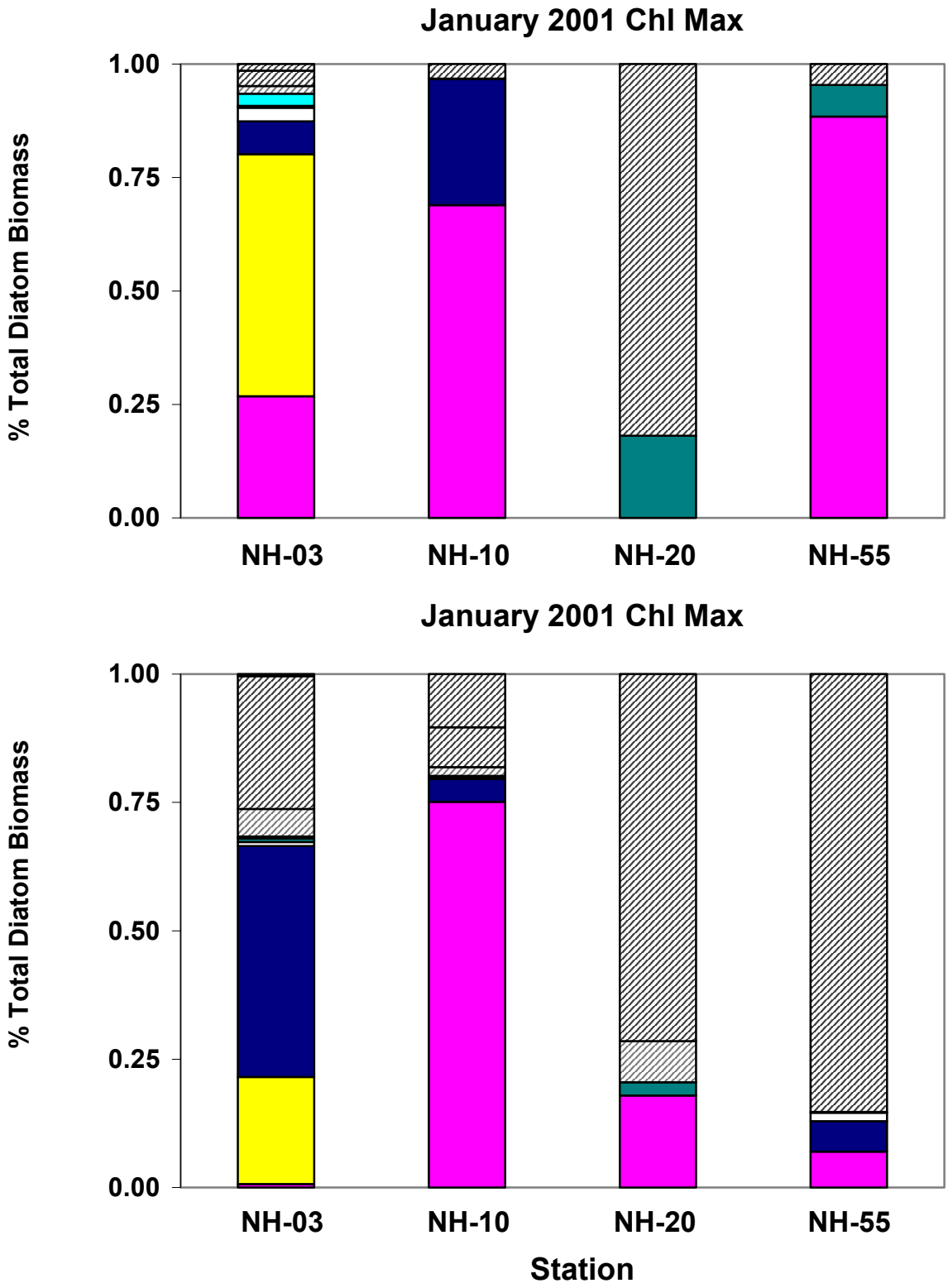

Figure 13: Winter (January 2001) across shelf distribution of major groups of diatoms in the surface and subsurface chl maxima as a percent of total diatom biomass. Refer to Figure 9 for legend.

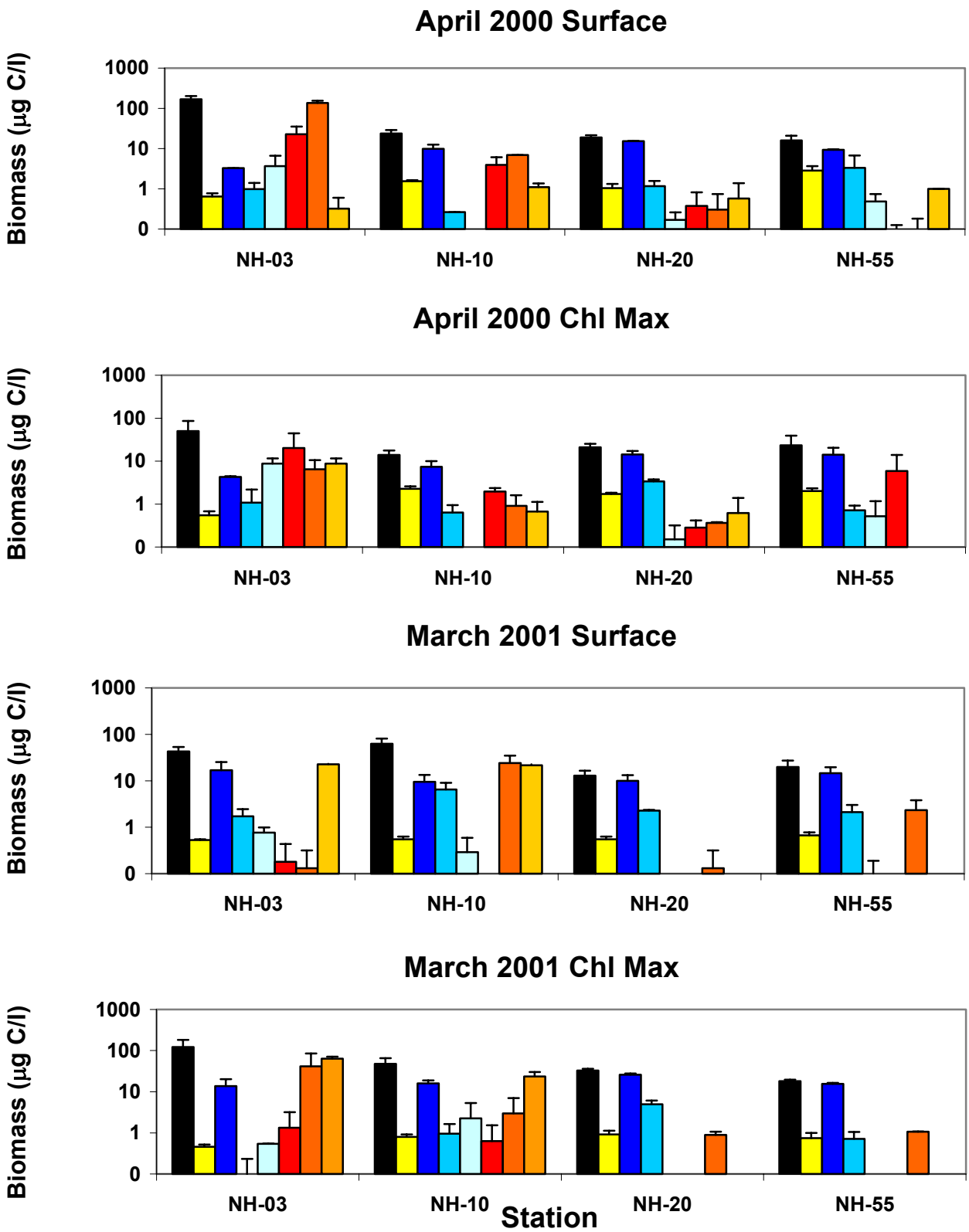

Figure 14: Spring (April 2000, March 2001) distribution of total phytoplankton biomass, cyanobacteria biomass, and the biomass of various sizes of flagellates and diatoms in both the surface and subsurface chl maximum. Error bars represent standard deviations between duplicate samples. Refer to Figure 8 for legend.

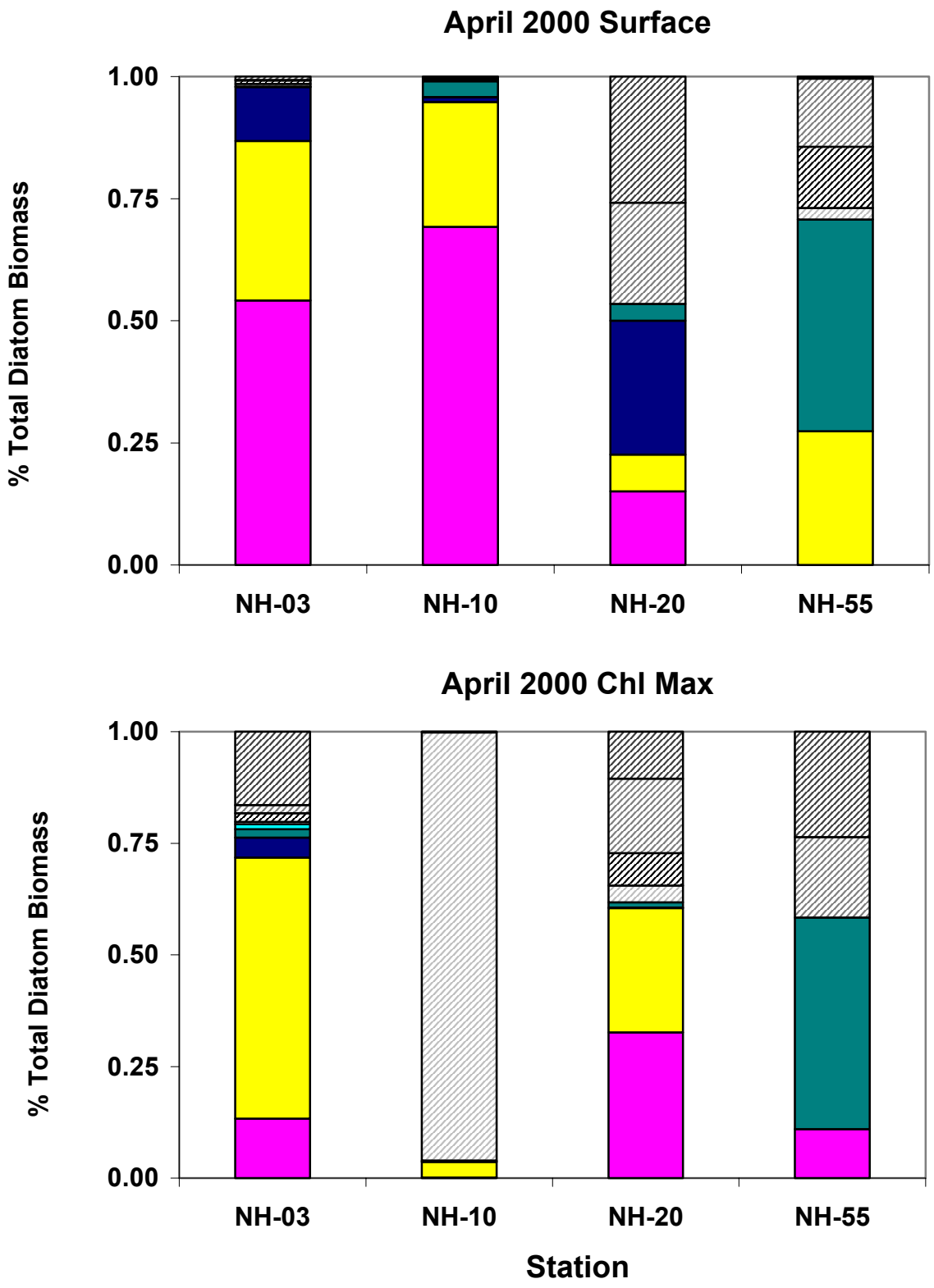

Figure 15: Spring (April 200,March 2001) across shelf distribution of major groups of diatoms in the surface and subsurface chl maximum as a percent of total diatom biomass. Refer to Figure 9 for legend.

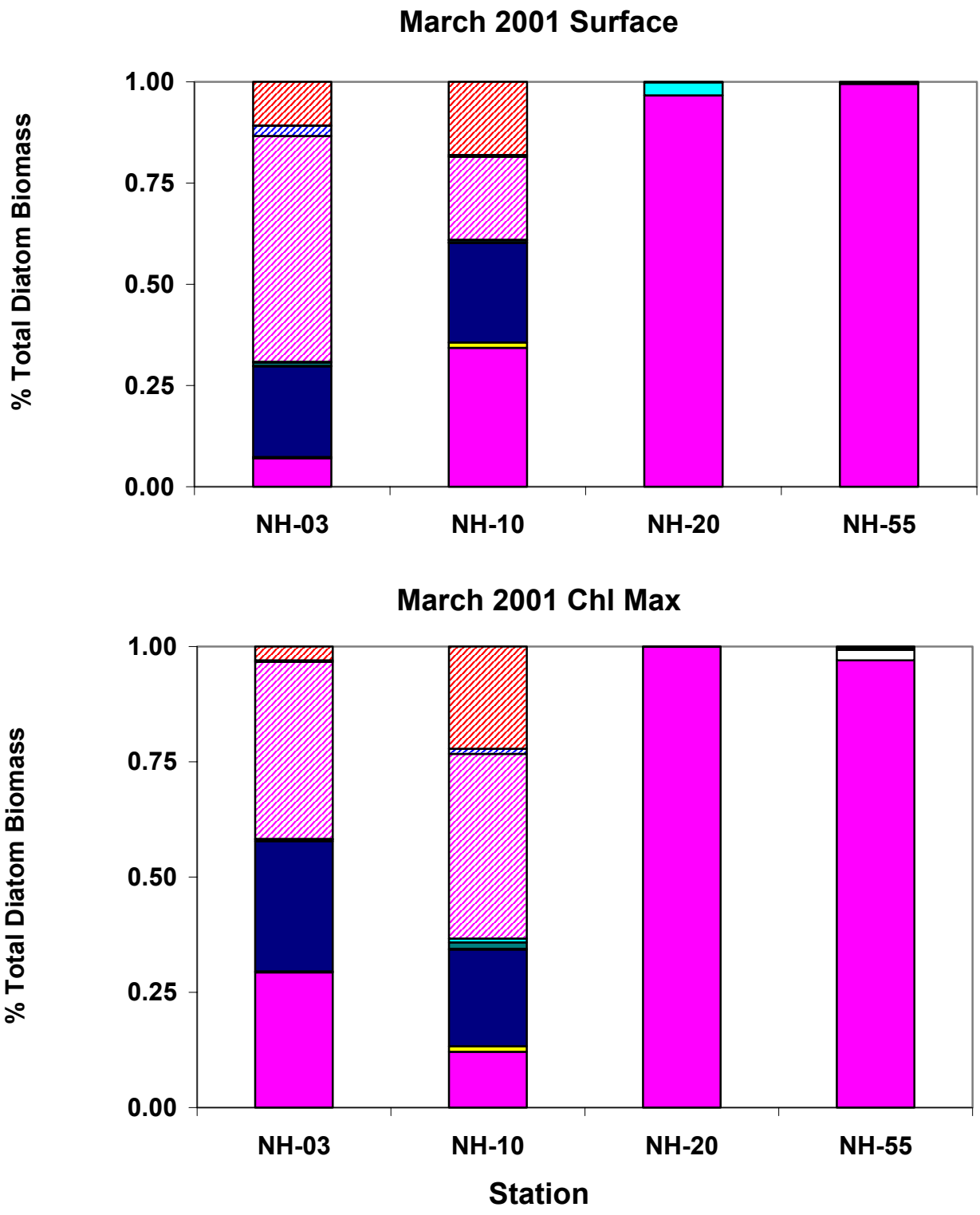

Figure 15 Cont'd

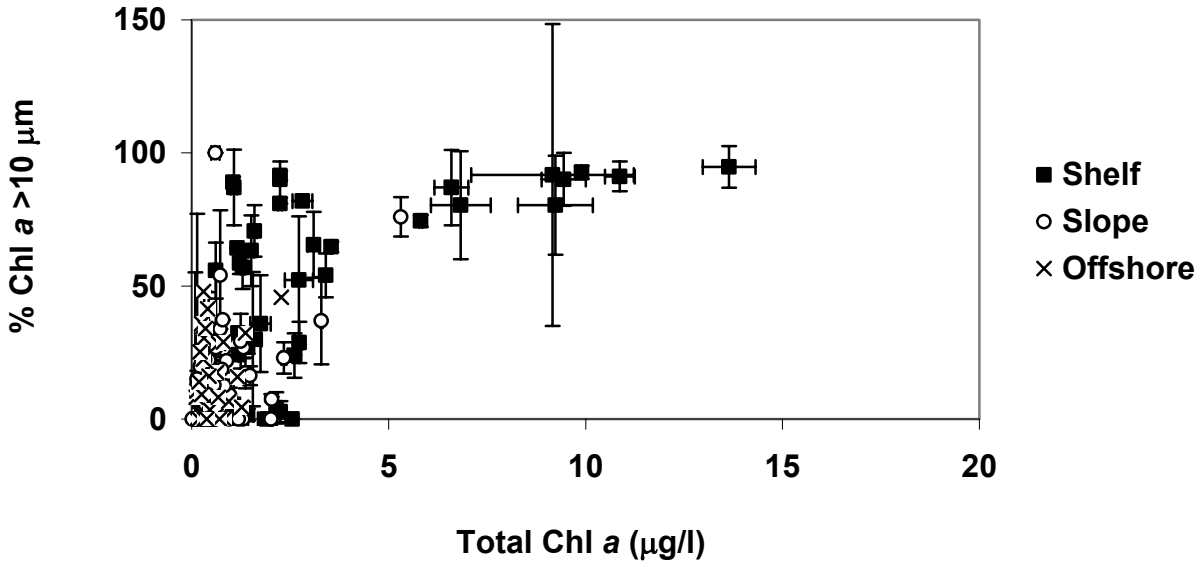

Figure 16: % Chl *a* >10 µm as a function of total Chl *a*, grouped by shelf, slope and offshore samples. Data represent summer (August 1998, July 1999, 2000 and 2001) and September (September 1998, 1999, 2000) cruises, and include all depths sampled for %Chl *a* >10µm (surface, 10m and subsurface chl maximum). Chl *a* error bars represent standard deviation of replicate measurements and % Chl *a* >10 µm error bars represent the standard deviation between the maximum and minimum estimates.

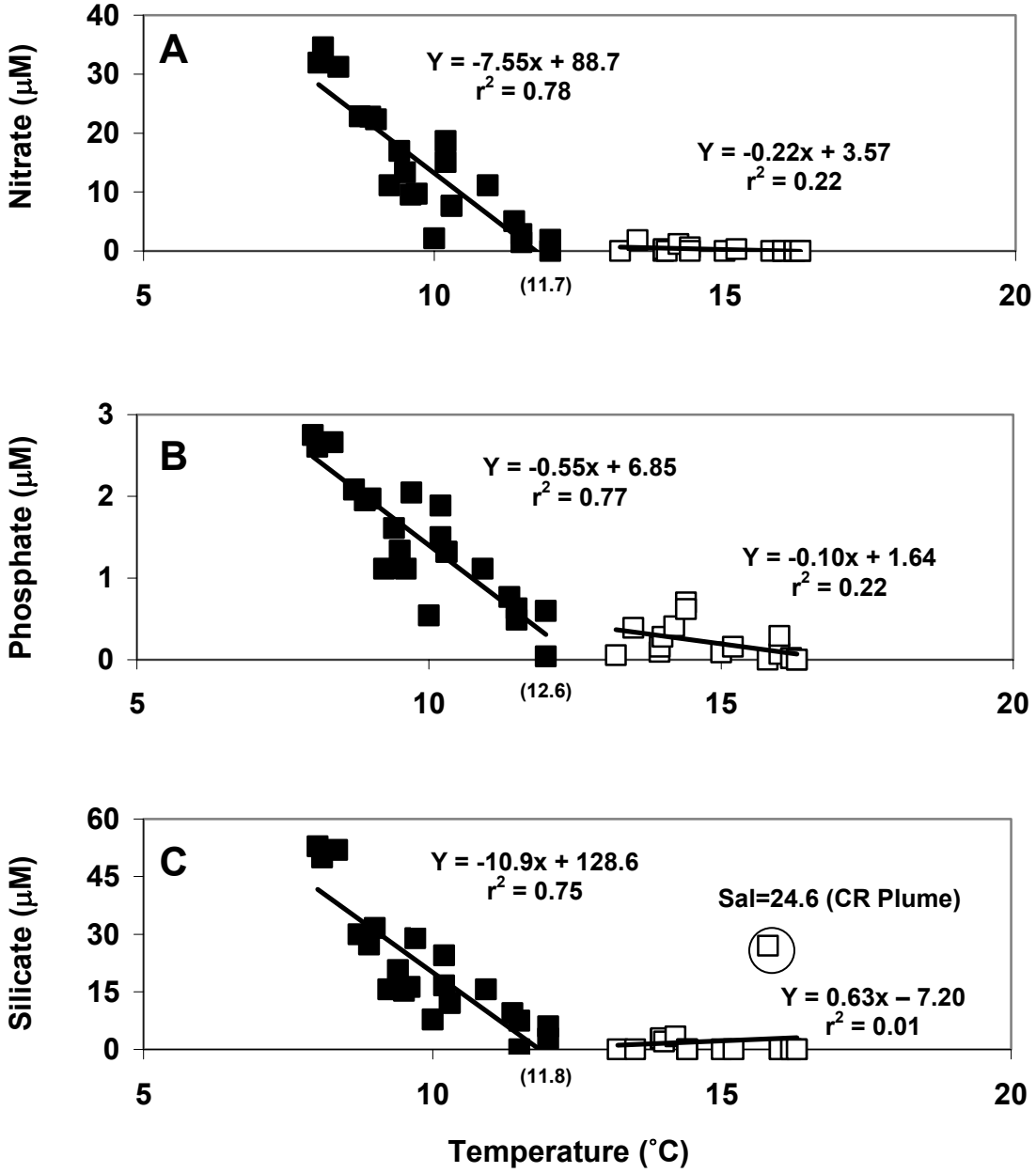

Figure 17: A. Nitrate B. Phosphate and C. Silicate concentrations as a function of temperature for summer and September shelf samples taken at the surface, 10m and subsurface chl maxima. The two linear regressions in each plot correspond to the part of the relationship in which nutrients are being depleted (filled squares) and then after they have been depleted (open squares). Numbers in parentheses indicate the intercept of the first linear regression, or the temperature above which that nutrient's concentration is zero or near zero. In part C, the circled point represents a surface sample from NH-05 during the July 2000 cruise and has a salinity of 24.6 psu. The NEP GLOBEC-LTOP cruise report indicates that it is part of the Columbia River plume. This cruise report can be found at http://globec.oce.orst.edu/groups/nep/reports/ccs_cruises/jul00cr.pdf

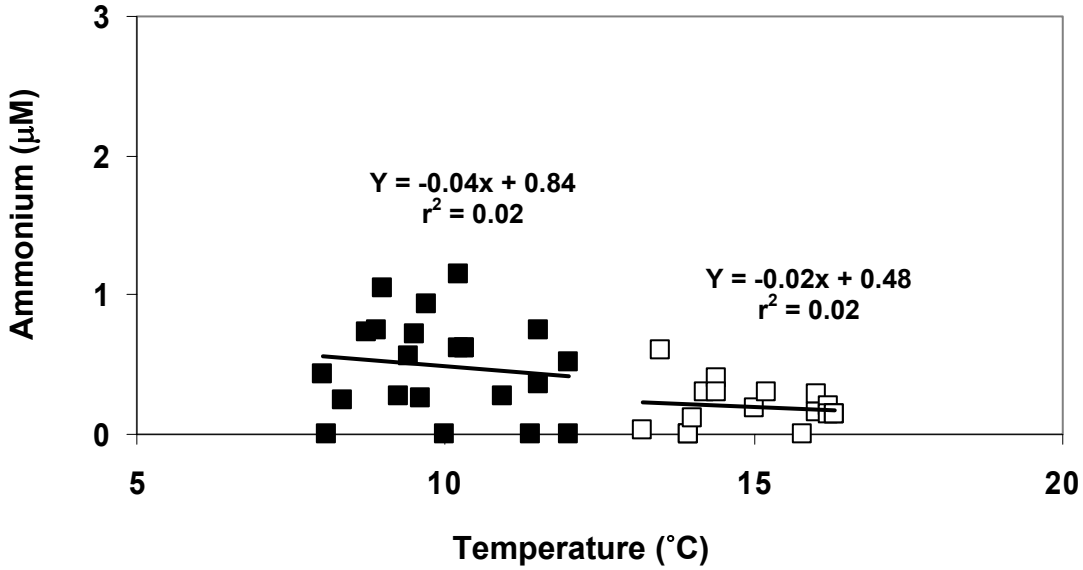

Figure 18: Ammonium concentrations as a function of temperature for summer and September shelf samples taken at the surface, 10m and subsurface chl maximum. The two linear regressions in each plot correspond to the part of the relationship in which nitrate, phosphate and silicate are being depleted (closed squares) and then after they have been depleted (open squares).

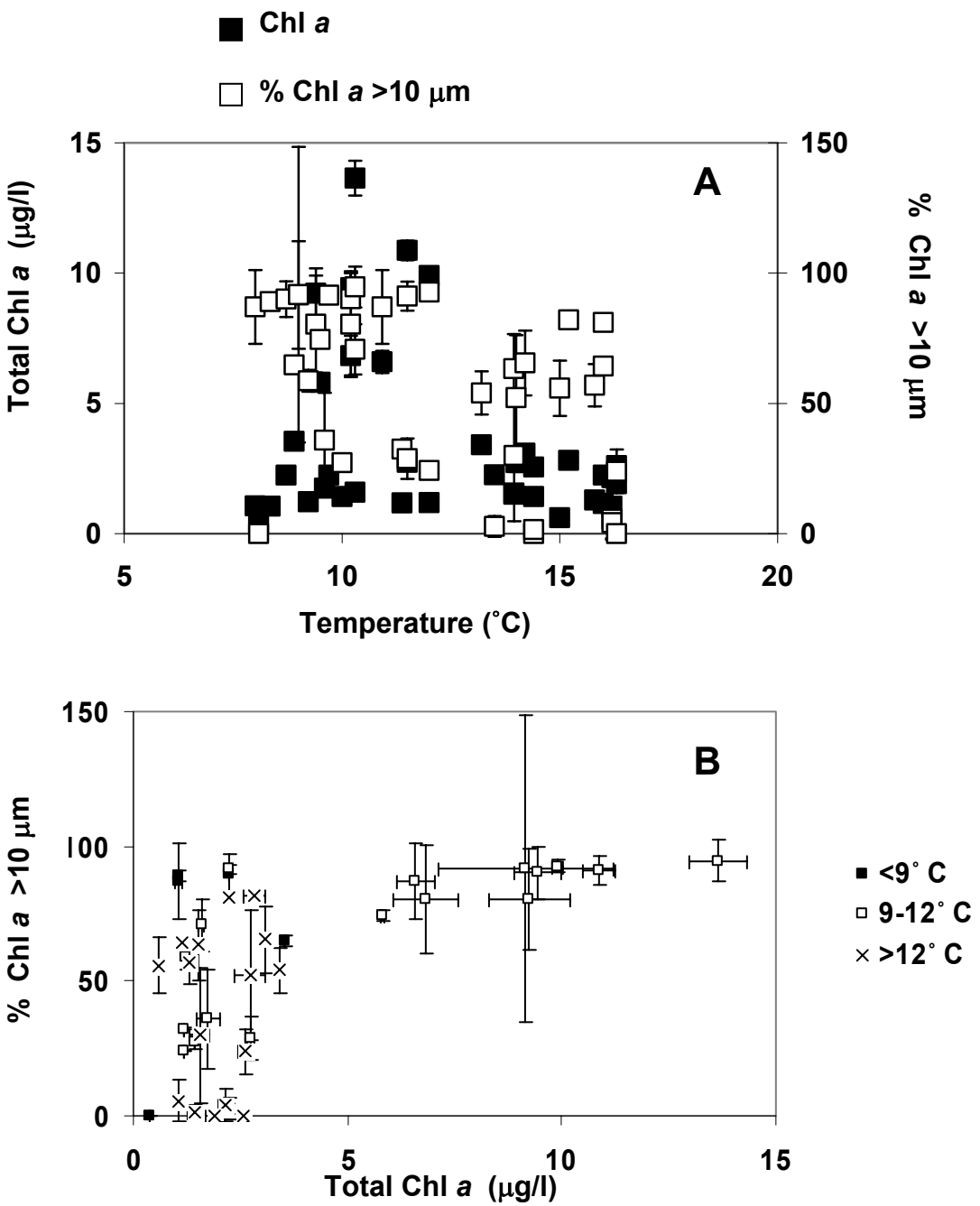

Figure 19: A. Total Chl *a* and % Chl *a* >10 μm as a function of temperature.
B. % Chl *a* >10 μm as a function of total Chl *a*, grouped by various temperatures. Temperature ranges are derived from the correlation of temperature with nitrate, phosphate and silicate for the same samples. Both plots represent summer and September shelf samples taken at the surface, 10m and subsurface chl maximum. Total Chl *a* error bars represent standard deviation of replicate measurements and % Chl *a* >10 μm error bars represent the standard deviation between the maximum and minimum estimates.

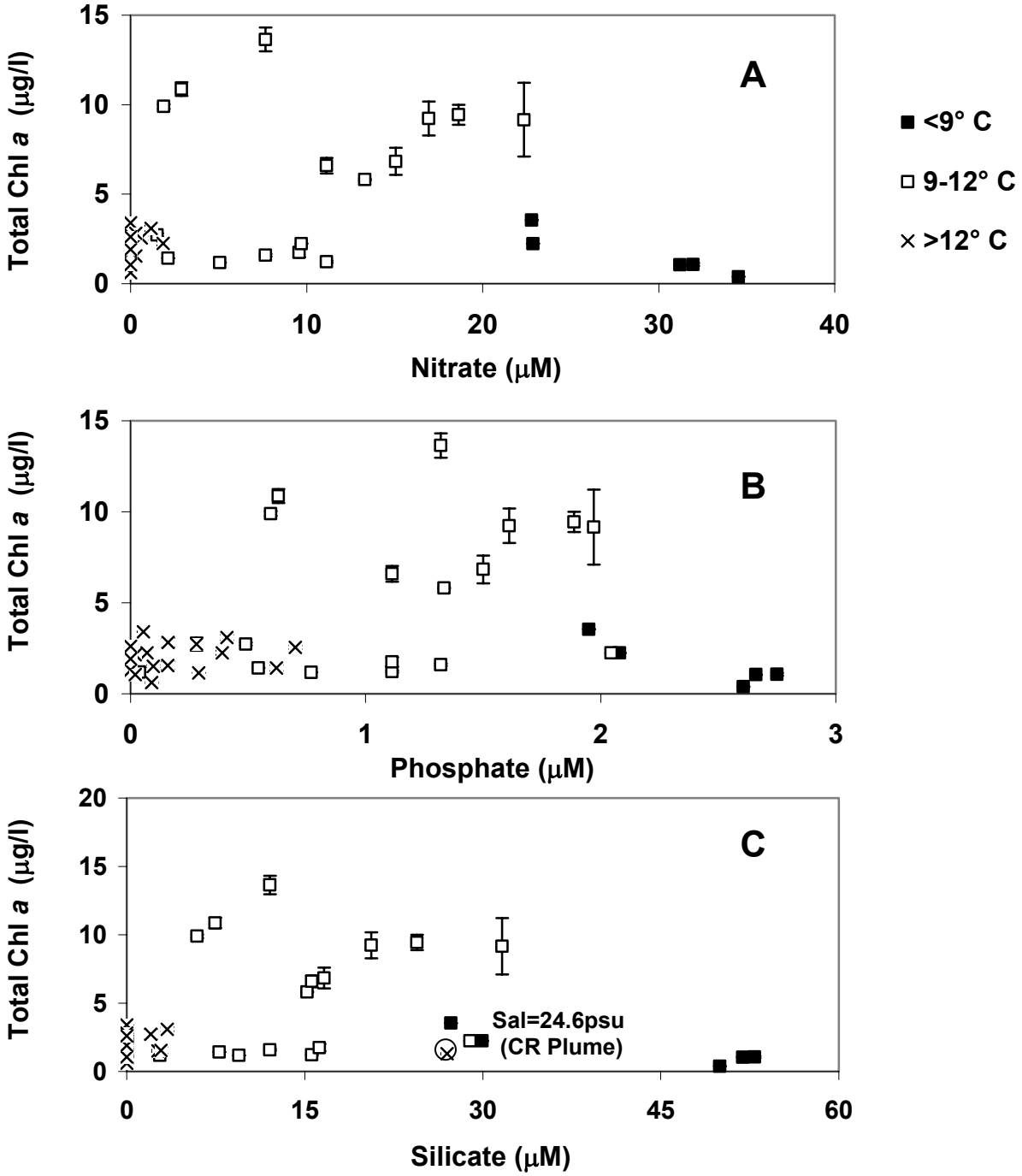

Figure 20: A. Nitrate B. Phosphate and C. Silicate concentrations vs. total Chl *a* for summer and September shelf samples taken at the surface, 10m and subsurface chl maximum. The data are grouped by various temperature ranges derived from the relationship between these nutrients and temperatures. Error bars represent standard deviations of replicate samples. In part C, the circled point represents a surface sample from NH-05 during the July 2000 cruise and has a salinity of 24.6 psu. The NEP GLOBEC-LTOP cruise report indicates that it is part of the Columbia River plume. This cruise report can be found at http://globec.oce.orst.edu/groups/nep/reports/ccs_cruises/jul00cr.pdf

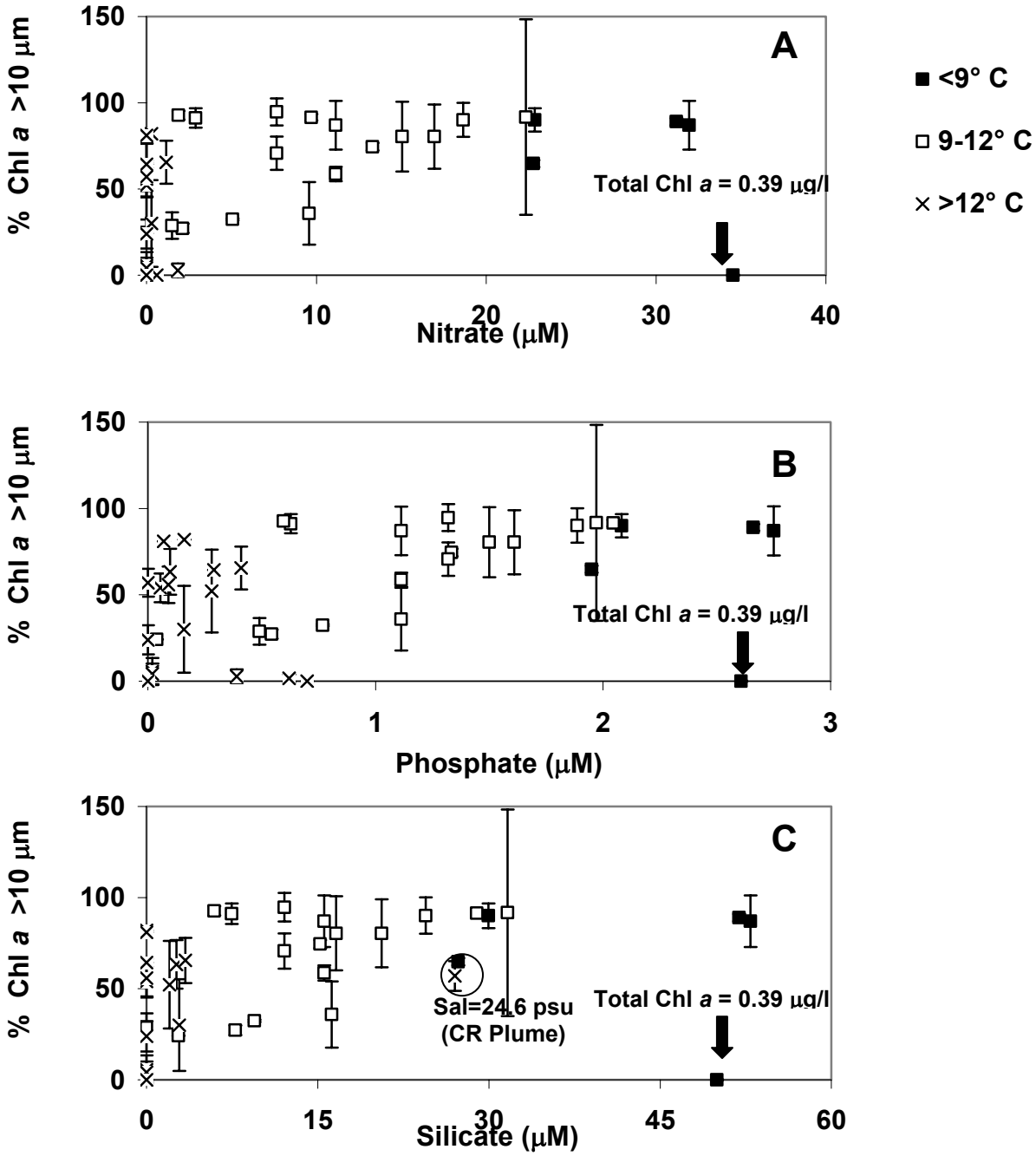

Figure 21: A. Nitrate B. Phosphate and C. Silicate concentrations vs. % Chl *a* >10 µm for summer and September shelf samples taken at the surface, 10m and subsurface chl maximum. The data are grouped by various temperature ranges derived from the relationship between these nutrients and temperature. The % Chl *a* >10 µm error bars represent the standard deviation between the maximum and minimum estimates. The arrow highlights a point of low Chl *a* that is addressed on page 27. In part C, the circled point represents a surface sample from NH-05 during the July 2000 cruise and has a salinity of 24.6 psu. The NEP GLOBEC-LTOP cruise report indicates that it is part of the Columbia River plume. This cruise report can be found at http://globec.oce.orst.edu/groups/nep/reports/ccs_cruises/jul00cr.pdf

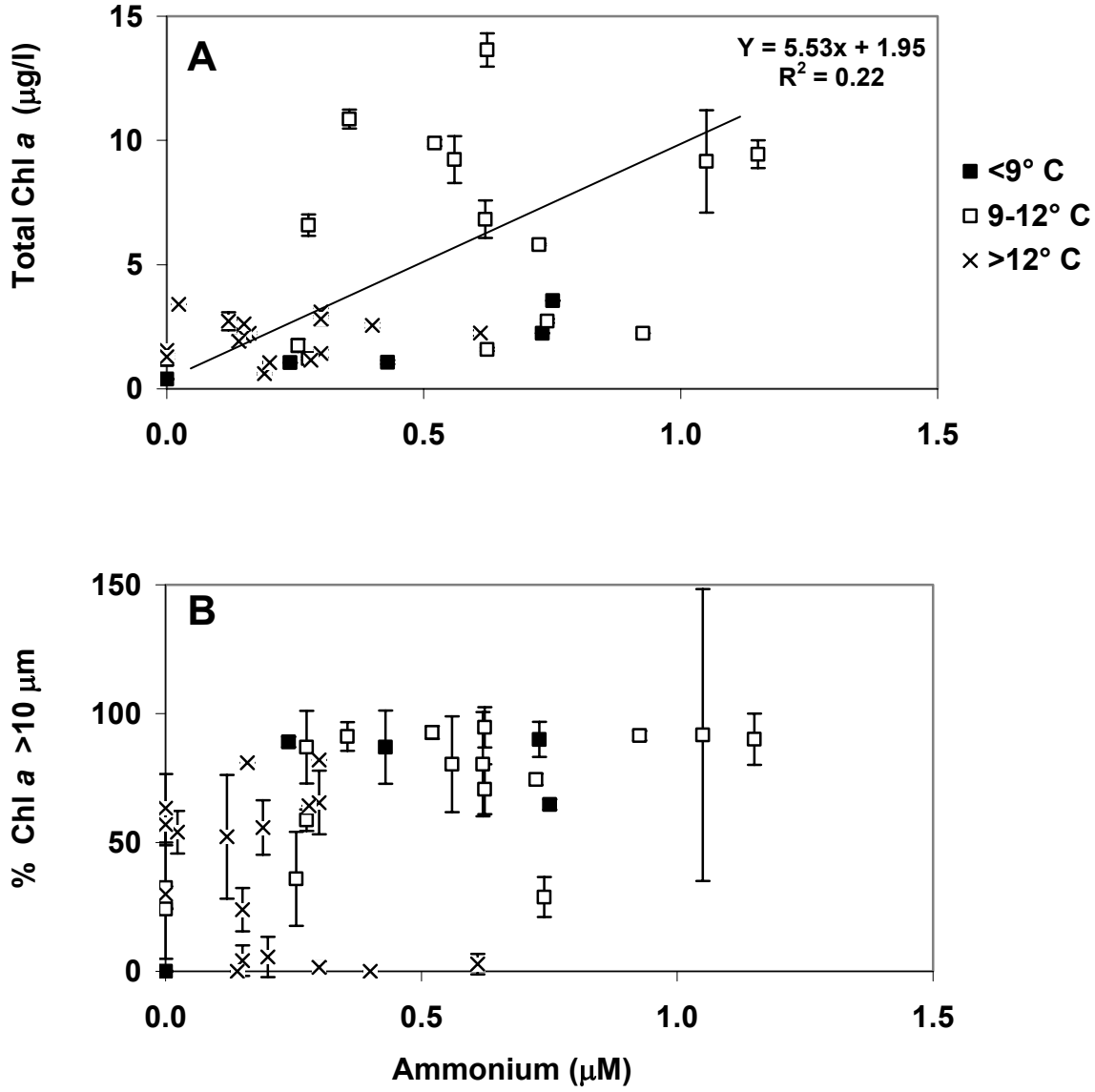

Figure 22: A. Total Chl *a* >10 µm and B. % Chl *a* >10 µm as a function of ammonium concentration for summer and September shelf samples taken at the surface, 10m and subsurface chl maximum. The data are grouped by various temperature ranges derived from the relationship between nitrate, phosphate, silicate and temperature. Total Chl *a* error bars represent standard deviations of replicate samples and % Chl *a* >10 µm error bars represent the standard deviation between the maximum and minimum estimates. The linear regression in part A corresponds to all points with temperatures ≤12˚ C.

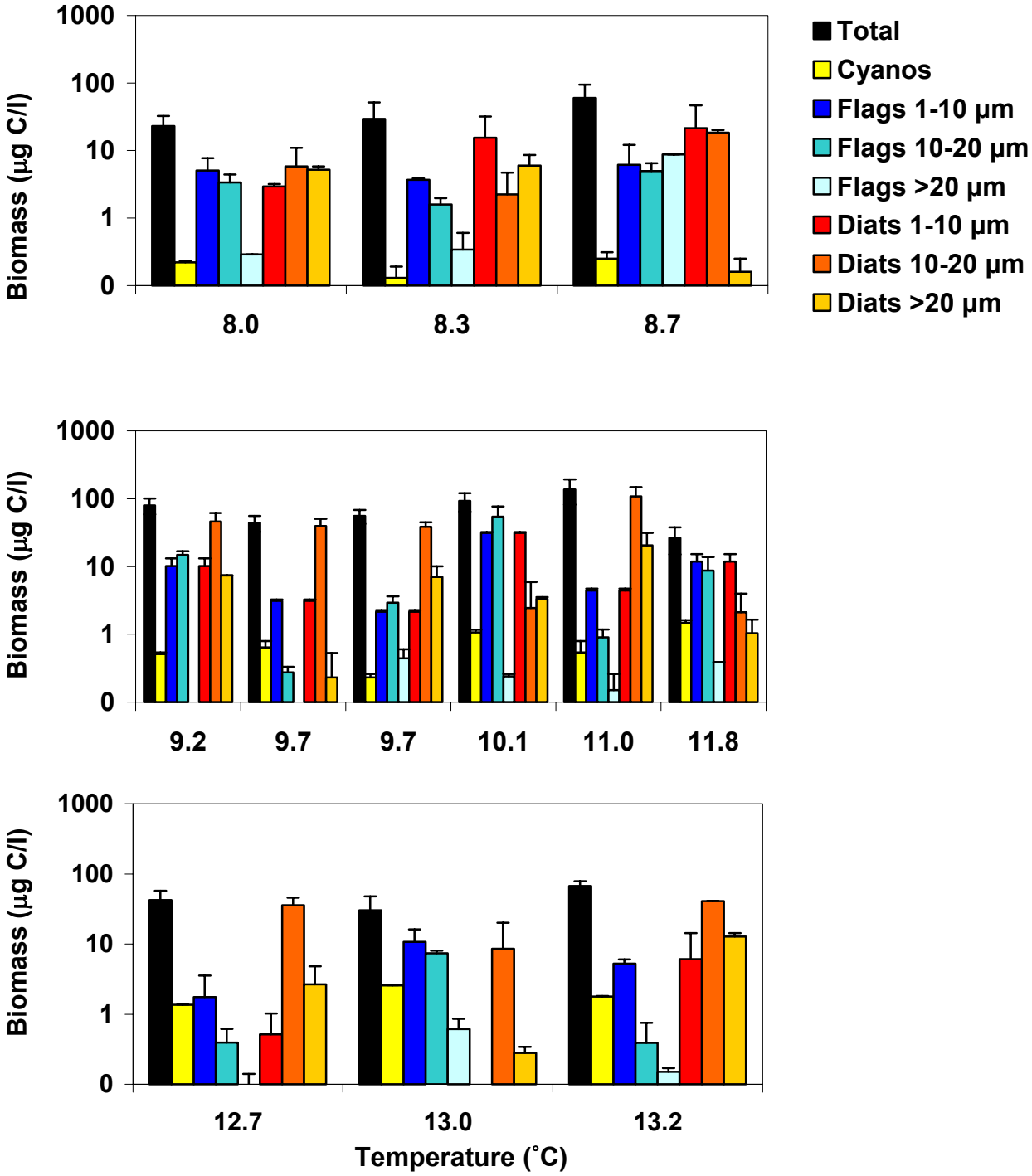

Figure 23: Distribution of total phytoplankton biomass, cyanobacteria biomass and the biomass of various sizes of flagellates and diatoms. Samples were collected during the September 2000, July 2000 and 2001 cruises from the surface and subsurface chl maximum of stations NH-03 and 10 and are grouped according to increasing temperature. Error bars represent standard deviations between replicate samples.

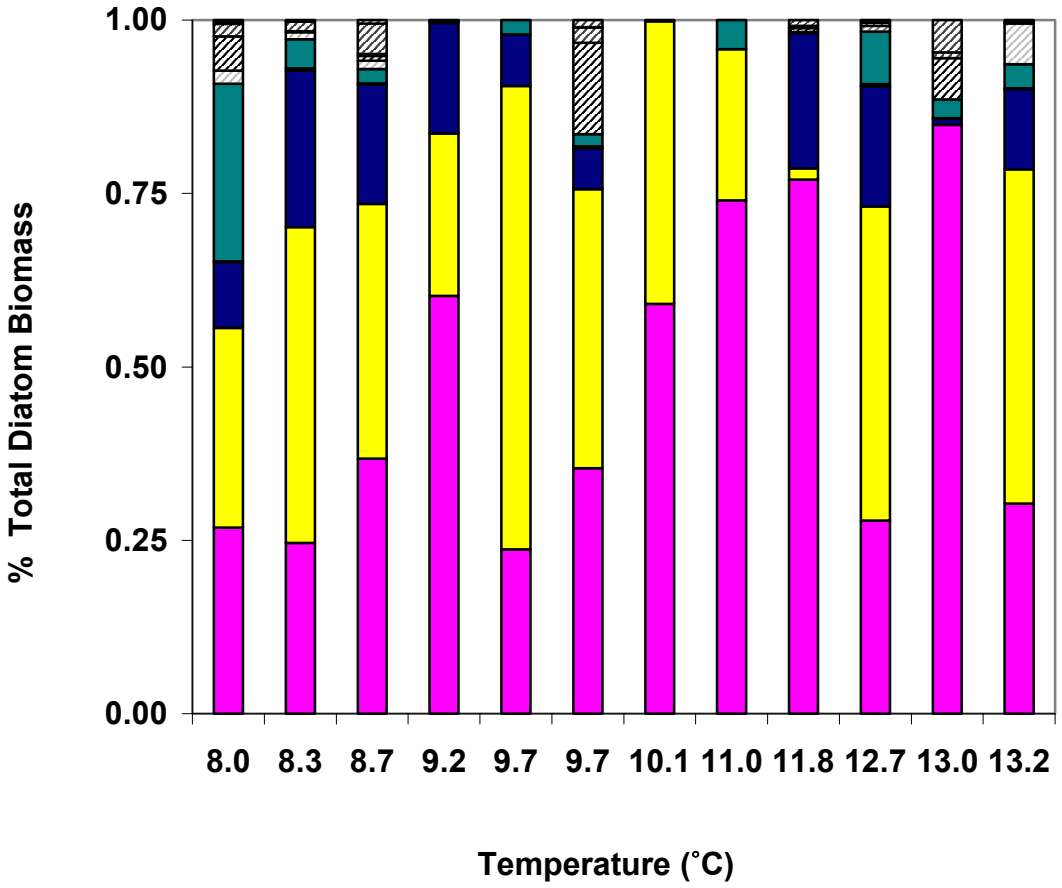

Figure 24: Distribution of major groups of diatoms as a percent of total diatom biomass, ordered with increasing sample temperature. Samples were collected during the September 2000, July 2000 and 2001 cruises from the surface and subsurface chl maximum of stations NH-03 and 10. Refer to Figure 9 for color legend.

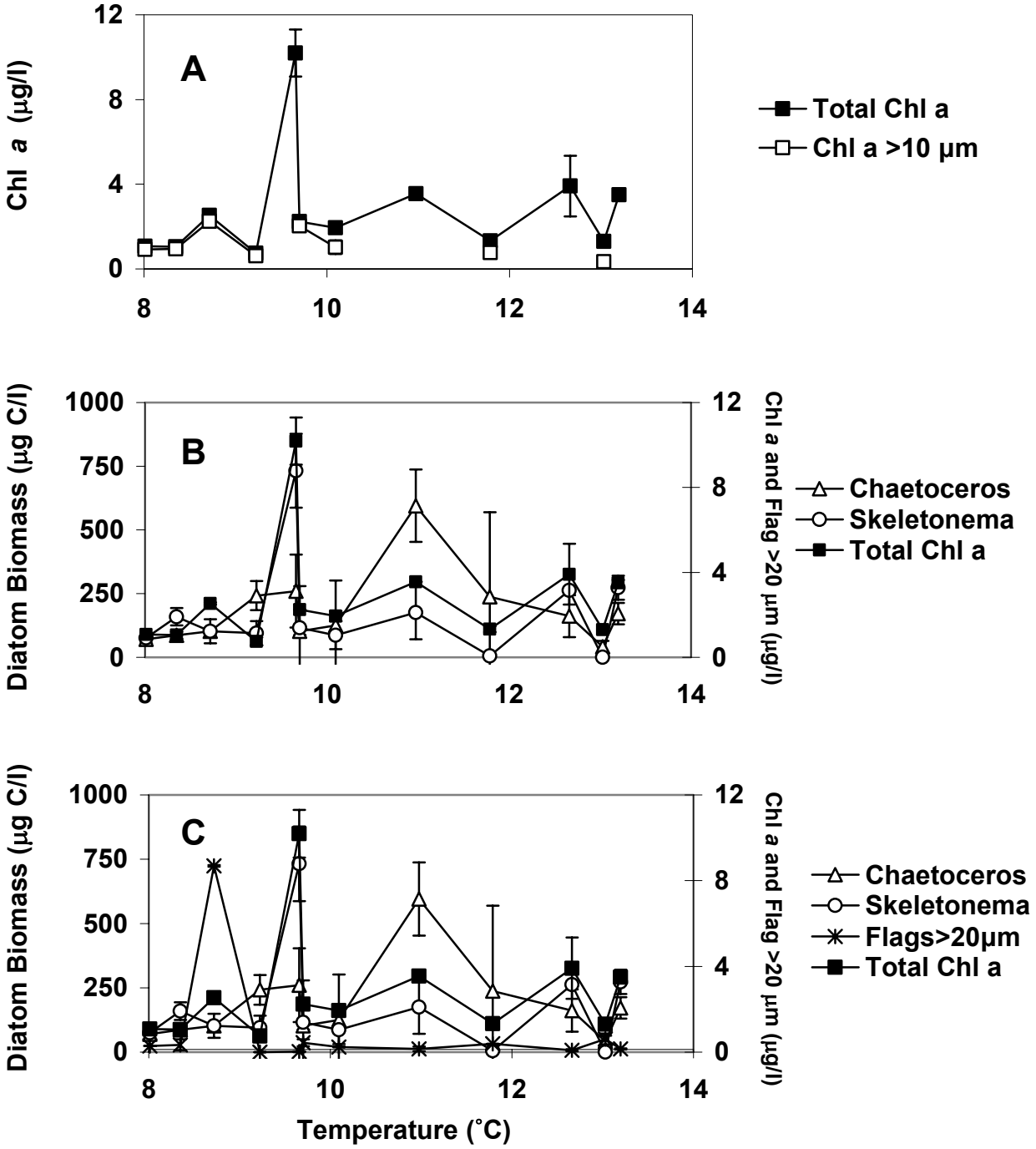

Figure 25: A. Total Chl *a* and Chl *a* >10 µm as a function of temperature B. Total Chl *a*, *Chaetoceros*, *Skeletonema* biomass as a function of temperature C. Same as B with flagellates >20 µm biomass added. Samples were collected during the September 2000, July 2000 and 2001 cruises from the surface and subsurface chlorophyll maxima of stations NH-03 and 10. Error bars represent the standard deviation between replicate samples.